The roles of Na$^+$ and K$^+$ in pyridoxal phosphate enzyme catalysis

Eilika U. Woehl, Michael F. Dunn*

Department of Biochemistry, University of California at Riverside, Riverside, CA 92521-0129, USA

Received 9 September 1994; in revised form 18 November 1994

Contents

---

* Corresponding author.

Abstract

The group I monovalent cations Na^+ and K^+ and ammonium ion are important effectors of catalytic activity for a wide variety of enzymes. Until recently, little was known about the mechanism of action of these effectors. However, in the past year, X-ray structures of three metal-ion-activated pyridoxal phosphate (PLP)-requiring enzymes have been solved. This information together with solution studies of these and related enzymes have provided new insights into the relationship between structure and function for monovalent cation-activated enzymes. By drawing on the extensive literature concerning the complexes formed between macrocyclic multidentate chelators and group I metal ions, this review examines the relationships between the properties of the metal ions, chelator affinity and binding specificity. This information is integrated with the structural information on the metal ion sites of monovalent-metal-ion-activated PLP enzymes and mechanistic hypotheses for the metal-ion-mediated interconversion of inactive and active forms of this class of enzymes. The available X-ray structures show in each case the active site(s) and the metal ion binding site(s) at distinctly separate loci. Consequently, in these systems the metal ion cofactor is properly classified as an allosteric effector that does not participate directly in bonding interactions with the reacting substrate. It is concluded that, under most physiological conditions, these effector sites are saturated, and binding of the metal ion is a permanent feature of catalysis. Given these constraints, two types of mechanism are considered to explain the effects of monovalent metal ions on catalytic activity: (1) mechanisms involving the metal ion in a static structural role wherein binding activates the enzyme by simply stabilizing the catalytically active conformation of the protein and (2) mechanisms where the metal ion plays a dynamic role in which binding selectively assists one or more of the protein conformational transitions essential for complementarity between enzyme site and the structure of an activated complex.

Keywords: Na^+; K^+; NH_4^+; Enzymes; Catalysis

1. Introduction

Monovalent cations, principally Na^-, K^+ and NH_4^+, are known to be important effectors of activity for more than 60 different enzymes. The subject of monovalent cation activation and/or inhibition has not been reviewed recently. Early reviews by Suelter [1,2] and by Evans and Sorger [3] documented the phenomena and offered some proposals for the functional roles played by monovalent metal ions. The motivation for preparing a review at this time which is focused on pyridoxal phosphate (PLP) enzyme systems has its origins in the advances made on two fronts: (a) the determination of the structures of the metal sites for three PLP enzymes, namely 2,2-dialkylglycine decarboxylase (DGD) [4,5], tyrosine phenol-lyase (TPL) [6–8] and tryptophanase [9,10] and (b) advances stemming from solution spectro-

scopic and mechanistic studies on these and related systems [11–31]. It has proven rather difficult to characterize the three-dimensional structures of the metal sites for Na^+ and K^+ in proteins because of the similarities in the X-ray scattering factors of these ions to water and hydronium ion (ten electrons). Na^+ has a scattering factor of 10 and K^+ has a scattering factor of 18. With refined, reasonably high resolution structures, it has been possible to locate the metal ion binding sites for Na^+ and K^+ in a few proteins [4–10,32–37]. These sites have been identified by strong spherical electron densities located in a cavity lined with donor atoms appropriately positioned to coordinate the metal. Characteristic bond lengths, B factors, difference electron density maps and isomorphous replacement with heavier monovalent metal ions have been particularly helpful for identifying sites for Na^+ and K^+ [4,5,32–37].

Rather than attempt to give a comprehensive review of the literature on monovalent cation binding proteins, this review presents mechanistic analyses of a select group of PLP enzymes for which a growing body of detailed information about structure–function relationships is developing. As appropriate, reference is made both to small molecule complexes and to other monovalent-metal-ion-activated (MMA) enzyme systems where some details of the structure–function relationship are known. Because of the specialized function played by Na^+–K^+ ATPases (ATP ≡ adenosine triphosphate) in the transport of monovalent cations across the plasma membrane, we exclude this class of enzyme from discussion in this review. While much remains unknown about the phenomenon of enzyme activation by monovalent metal ions, one objective of this review is to stimulate interest in this neglected area of research.

For a variety of reasons, the mechanistic literature concerning the roles played by coenzymes in enzyme catalysis is unusually rich in chemical detail. Coenzymes frequently provide distinctive spectroscopic signatures that facilitate the study of mechanism. For the past 30 years, through "chemical mutagenesis" it has been possible to alter the coenzyme structure and therefore the chemical reactivity in ways that have only recently become available, via the tools of molecular biology, to modify the protein structure. For these reasons, it is well known that coenzymes facilitate catalysis through specific bonding interactions with the reacting substrate, or in the case of redox enzymes as redox centers that undergo changes in oxidation state as substrate is oxidized or reduced [38].

The category of effectors of enzyme function known as cofactors is a more diverse collection of molecules and ions that affect enzyme activity via a wide variety of mechanisms, including (a) direct bonding interactions with the reacting substrate (e.g. zinc metalloenzymes) [38–41], (b) allosteric interactions that modulate protein function through ligand binding at distant sites (usually on different subunits) [42] and (c) molecules or ions that modify protein structure and/or activity by interactions on the same polypeptide chain as the active site but at separate loci [43–48,49]. As a class, the mechanisms by which cofactors influence enzyme catalysis and protein function are probably less well understood than the chemistry and mechanisms by which coenzymes act.

The emerging literature on the structure and action of monovalent-cation-requiring enzymes indicates that in most instances these ions should be classified as cofactors that act through binding interactions at sites distinctly separate from the catalytic

site, but which are located on the same subunit [4–10,34]. For example, the recently published structural work on the pyruvate kinase K^+ site shows that this metal ion binds 6–8 Å away from the catalytic site [34]. In some systems (e.g. tryptophan synthase), monovalent metal ions exhibit both intrasubunit and intersubunit interactions that are important to the function of the protein [28–31]. The modulation of protein function by the action of monovalent cations therefore falls under the broad classification of allosteric ("other site") interactions wherein binding to one site affects the properties of a distant site. For the majority of enzymes in this class, the function of this allostery appears not to be tied to the regulation of metabolic pathways or enzyme cascades. Catalytic activity appears not to be modulated in these systems by in-vivo fluctuations in metal ion concentration [1,2,28–31,50,51]. The dissociation constants for Na^+ or K^+ binding usually are well below the physiological concentrations of these ions. Therefore these binding sites are saturated, and binding of the metal ion is a permanent feature of catalysis [50].

If the metal ion sites of MMA enzymes are always saturated under physiological conditions, then the roles played by these metal sites are most probably linked to events that occur during the catalytic cycle. This linkage has been explored in most systems by simply comparing the effects of metal ion removal on the catalytic properties of the enzyme. This comparison usually has been restricted to consideration of steady state kinetic parameters and/or ligand affinities [11–17,19,21,24,51–56]. In a few instances, this comparison has been extended to detailed analysis of the effects of the monovalent metal ion on individual steps in the chemical mechanism of the enzyme-catalyzed reaction [20,22,23,26–31,50].

2. Roles of monovalent cations in enzyme catalysis

Possible mechanisms by which monovalent cations alter catalysis for the class of MMA enzymes considered in this review are discussed below. This discussion is restricted to systems where the bound cation can be considered a permanent feature of catalysis, and the metal site is distant from the catalytic site. Therefore direct interactions between metal ion and substrate are eliminated from consideration. Two broad categories of mechanism are then likely to be relevant: (a) those where the monovalent metal ion primarily plays a structural role and (b) those where the monovalent metal ion plays a more dynamic role. Both categories of mechanism must have protein conformational origins.

2.1. Structural roles

The most simplistic and obvious role for the metal ion in MMA enzyme catalysis is that the metal ion site is a structural element, not unlike a disulfide cross-link or salt bridge, which functions to stabilize an active conformation of the enzyme. Cation

binding to this site drives the protein from a less active, or essentially inactive, conformation (E_i) to a conformation with high catalytic activity (E_a):

$$
E_i + M^+ \; \rightleftharpoons \; (M^+)E_a \; \overset{S}{\rightleftharpoons} \; (M^+)E_a(S)
$$

$$
(M^+)E_a(P) \rightleftharpoons \; \cdots \; \rightleftharpoons (M^+)E_a(X)
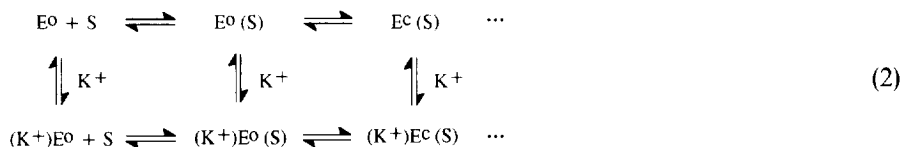$$

(1)
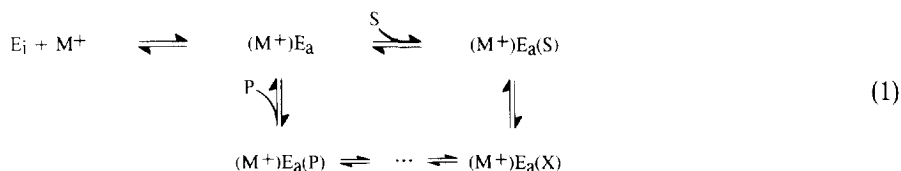
Such a conformational transition results in altered substrate specificity (as measured by k_{cat}/K_m), reflecting changes in either k_{cat} or K_m or in both. A useful analogy is the hydrogen-ion-induced alteration in K_m values for α-chymotrypsin substrates resulting from protonation of the α-amino group of Ile16, a component of the salt bridge that stabilizes the high affinity form of the enzyme [57–59].

If metal ion binding simply shifts the distribution of pre-existing enzyme forms, then the details of the catalytic mechanism are not really altered; the only change is in the distribution of forms with different activities (e.g. the above-mentioned proton activation of α-chymotrypsin). However, if metal ion binding induces the formation of a new protein conformation, then the details of catalysis may be altered such that a new energy surface is transversed with altered transition states for the interconversion of intermediates along the reaction path. The enhancement of catalysis by this mechanism would correspond to a Pauling strain distortion effect [38,57,60,61] wherein metal ion binding drives the protein to a conformation with improved complementarity to the transition state of the rate-limiting chemical step. These alterations in mechanism could be subtle or large, depending on the nature of the conformational transition and its effects on bonding in the transition state.
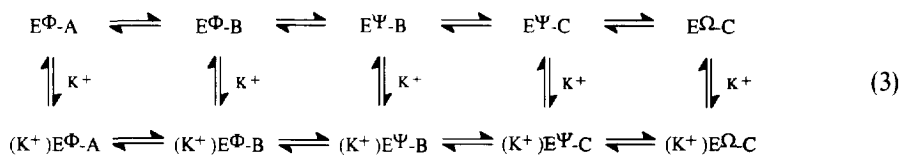
One consequence of a metal-ion-induced shift in the distribution of inactive and active forms of the enzyme towards the active form simply could be a change in substrate affinity for the enzyme. Many enzymes are now known to undergo a conformational transition between "open" and "closed" conformations during the catalytic cycle [62–74]. In these systems, the designations "open" and "closed" refer to the accessibility of the catalytic site to substrate and solvent molecules. The closed conformations usually correspond to the catalytically active forms of bound substrate and, in these complexes, substrate is usually sequestered away from any contact with solvent. In contrast, the open conformation allows easy access of substrate and solvent molecules into the site. Because there is no obvious route for substrate entry into the closed conformation, it is assumed that binding is a two-step process in which substrate first binds to the open conformation and this initial complex undergoes the conformational transition to the closed structure. Of course, this sequence must be reversed at some point further along in the catalytic cycle so that product(s) may be released. One possible role for monovalent metal ions is the modulation of the conformational transition between open and closed conformations of MMA enzymes that undergo this structural transition as part of the catalytic cycle. A hypothetical example employing K^+ as the activating monovalent cation is as follows:

$$E^O + S \rightleftharpoons E^O(S) \rightleftharpoons E^c(S) \quad \cdots$$
$$\Big\updownarrow K^+ \qquad \Big\updownarrow K^+ \qquad \Big\updownarrow K^+ \qquad\qquad (2)$$
$$(K^+)E^O + S \rightleftharpoons (K^+)E^O(S) \rightleftharpoons (K^+)E^c(S) \quad \cdots$$

If the metal ion binds more tightly to one or the other of the two conformational states, then binding will shift the distribution between open and closed conformers. In the example shown in Eq. (2), E^o and E^c refer to the open and closed conformations of the enzyme.

2.2. Dynamic roles

Pauling's strain distortion hypothesis for enzyme catalysis [60,61] proposes that complementarity between the structure of the enzyme site and the structure of the activated complex is responsible for the lowering of the activation energies of enzyme-catalyzed chemical transformations. This thermodynamic truism offers a satisfying picture that explains some facets of catalysis, provided that the reaction pathway occurs via a single chemical transformation. For systems that involve multiple chemical transformations (e.g. PLP enzymes), it is not obvious how the enzyme site can be complementary to each activated complex along the pathway unless the structure of the site can adapt to the structure of each activated complex [75,76]. For this to occur, it then becomes logical to propose that the enzyme exists as an ensemble of conformations which includes structures that are complementary to each of the transition states [75,76]. If this picture of enzyme catalysis has congruence with reality, then cofactor binding could provide a driving force that assists one or more of the protein conformational transitions necessary to achieve complementarity between the site structure and the structure of an activated complex. Thus monovalent metal ion binding could selectively lower the activation energy for a particular step, provided that the metal ion binds more tightly to the conformation of the protein that is complementary to the structure of the transition state for that step. One such scheme is given by

$$E^\Phi\text{-}A \rightleftharpoons E^\Phi\text{-}B \rightleftharpoons E^\Psi\text{-}B \rightleftharpoons E^\Psi\text{-}C \rightleftharpoons E^\Omega\text{-}C$$
$$\Big\updownarrow K^+ \quad \Big\updownarrow K^+ \quad \Big\updownarrow K^+ \quad \Big\updownarrow K^+ \quad \Big\updownarrow K^+ \qquad (3)$$
$$(K^+)E^\Phi\text{-}A \rightleftharpoons (K^+)E^\Phi\text{-}B \rightleftharpoons (K^+)E^\Psi\text{-}B \rightleftharpoons (K^+)E^\Psi\text{-}C \rightleftharpoons (K^+)E^\Omega\text{-}C$$

and is shown in Fig. 1 for a system that is subject to activation by K^+.

In Eq. (3), A, B and C are enzyme-bound covalent intermediates which lie along the reaction path. E^Φ, E^Ψ and E^Ω are the enzyme conformations that are complementary to the transition states for the interconversion of A to B, of B to C and of C to the following intermediate, respectively. If K^+ binds more tightly to E^Ψ than to E^Φ or E^Ω, then K^+ binding selectively lowers the free energies of all forms of E^Ψ. If interconversion of E^Ψ–B and E^Ψ–C is rate determining for the overall transformation,
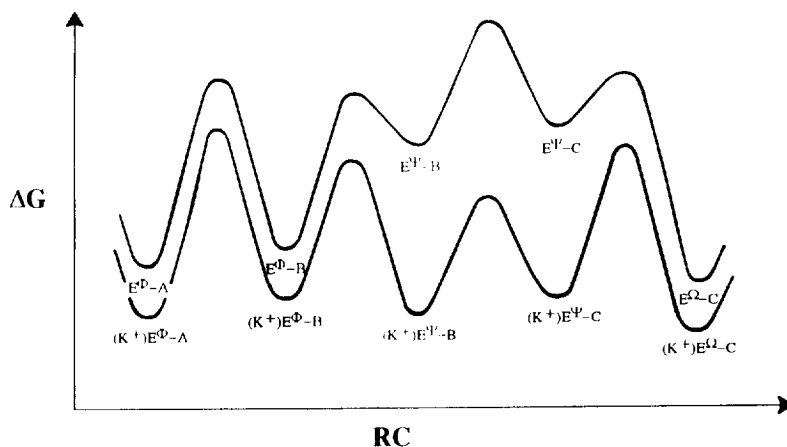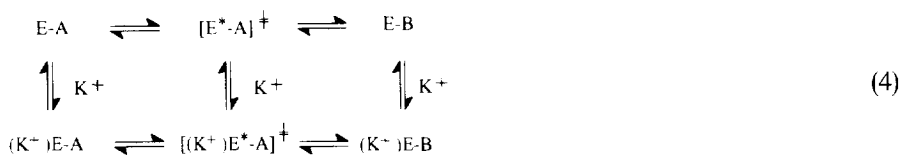
Fig. 1. Free-energy–reaction coordinate (RC) diagrams corresponding to the processes depicted in Eq. (3), showing the effects of K^+ on the relative energies of ground states and transition states for the case where K^+ binds with higher affinity to the enzyme conformation E^Ψ than to the conformations designated E^Φ and E^Ω. The preferential binding of K^+ to E^Ψ lowers the activation energy for this sequence of transformations and brings about a change in the rate-determining step.

and if the free energies of the E^Ψ–B and E^Ψ–C ground states are higher than either E^Φ–A or E^Ω–C, then K^+ binding will lower the activation energy of the rate-determining step, and the rate of turn-over will be increased. In certain circumstances, the binding of the metal ion could change the rate determining step. The free-energy diagram for such a system is depicted in Fig. 1.

The differences between the free energies of each ground state and each activated complex depicted in Fig. 1 are determined by the strengths of the bonding interactions between (i) the site and the bound substrate structure (ground-state or activated complex), (ii) the metal ion and the protein, (iii) the interresidue interactions for each protein conformation and the activation energies for each process. Therefore the activating interactions due to metal ion binding could be operative in more than one step. The selective binding of metal ion to certain protein-bound intermediate states will bring about a different distribution of enzyme-bound intermediates (both in the steady state and at equilibrium) in comparison with the distributions characteristic of the metal-free enzyme. Thus, if this mechanism plays a significant role in MMA enzymes, then both the rates of individual processes and the distribution of catalytic intermediates along the reaction pathway should be different for the metal-free and metal-bound enzymes. The extent to which the overall pathway is affected will be determined by the differences between the affinities of the metal ion for the different conformations along the pathway.

A variation of the mechanism presented in Eq. (3) that would lead to selective catalytic enhancement of some steps over others is given by

$$\begin{array}{ccccc}
\text{E-A} & \rightleftharpoons & [\text{E}^*\text{-A}]^{\ddagger} & \rightleftharpoons & \text{E-B} \\
\Big\updownarrow \text{K}^+ & & \Big\updownarrow \text{K}^+ & & \Big\updownarrow \text{K}^+ \\
(\text{K}^+)\text{E-A} & \rightleftharpoons & [(\text{K}^+)\text{E}^*\text{-A}]^{\ddagger} & \rightleftharpoons & (\text{K}^+)\text{E-B}
\end{array} \qquad (4)$$

and is shown in Fig. 2. In this system, the enzyme undergoes conformational transitions during each chemical step such that the conformation of the protein in the transition state (E^* species in Eq. (4)) is complementary to the structure of the activated complex. If K^+ binds more tightly to $[\text{E}^*\text{-A}]^{\#}$ than to either E–A or E–B, then the activation energy for interconversion of $(\text{K}^+)\text{E-A}$ and $(\text{K}^+)\text{E-B}$ will be lower than the activation energy for interconversion of E–A and E–B. Here, the change $\Delta(\Delta G^{\#})$ in $\Delta G^{\#}$ is a direct measure of the difference between the affinities of the ground state and transition state for K^+; hence, $\Delta(\Delta G^{\#}) = -RT \ln(K_D^{TS}/K_D^{GS})$, where K_D^{TS} and K_D^{GS} are the dissociation constants for K^+ binding to the transition state and to the ground state respectively. If the increased affinity of K^+ for the transition state occurs only in certain transition states along the reaction path, then only those steps where the affinity is increased will exhibit lowered activation energies when K^- is bound.

Escherichia coli homoserine dehydrogenase-1 (HD-1) is an interesting example of an allosteric enzyme that is subject to strong activation by K^+ and slight inhibition by Na^+ [51]. The action of the allosteric feedback inhibitor, L-Thr, resembles some of the effects of Na^+ on the properties of the enzyme. L-Thr binding shifts the enzyme forms toward a low activity form, a T state, in which only the rate of the chemical interconversion of ternary complexes is reduced. Na^- also appears to stabilize this
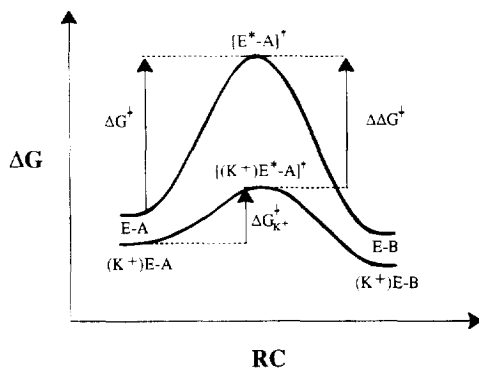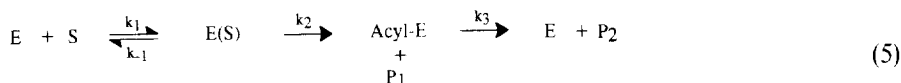

Fig. 2. Free-energy–reaction coordinate (RC) diagram for the reaction sequence shown in Eq. (4). In this case, the enzyme undergoes a conformational transition as the transition state is formed such that the conformation of the catalytic site is complementary to the structure of the activated complex. The diagram shows the case where K^+ binds more tightly to the protein conformation in the transition state than to either ground state (E–A or E–B). As is evident from comparison of the two energy surfaces, preferential binding to the transition state can significantly lower the activation energy for the chemical transformation. The free-energy change $\Delta(\Delta G^{\#})$ is a measure of the free energy for the binding of K^+ to the transition state.

T state. However, K^+ activation modifies both the rates of chemical processes and the rates of substrate binding and dissociation steps along the catalytic pathway. Equilibrium isotope exchange kinetic studies of HD-1 [51] show that, relative to Na^+, K^+ activates the catalytic interconversion of the enzyme ternary complexes of substrates and products (EAB with EPQ) fortyfold, increases the rate of substrate–product dissociation from the ternary complexes twentyfold, while increasing the affinity of the dead-end complex EQA seventeenfold. Wedler and Ley [51] have shown that the properties of the system make it unlikely that K^+ interacts directly with substrate or coenzyme at the active site. The behavior of HD-1 is consistent with a mechanism wherein the ground-state energies and the activation energies of some steps are altered by monovalent metal ion binding.

Human α-thrombin provides an important example of an Na^+-activated enzyme. While most MMA enzymes are activated by K^+, thrombin shows a preference for activation by Na^+. Wells and Di Cera [50] have argued that the specificity for Na^+ reflects the conditions found in the blood stream where thrombin functions in vivo. The extracellular environment of blood is high in Na^+ and lower in K^+. Therefore Wells and Di Cera [50] argue that the specificity for Na^+ has been tailored to these conditions. These workers have investigated the effects of monovalent metal ions both on the physical properties of the protein and on individual steps of the thrombin catalytic mechanism. They found that the intrinsic fluorescence of the enzyme is increased by more than 20% when Na^+ (or K^+) is bound, a clear indication that metal ion binding triggers a significant change in protein conformation. The enhancement of fluorescence was found to parallel Na^- induced changes in the catalytic behavior of the enzyme, indicating that a single metal ion binding locus is responsible for both. Like other serine proteases, the steady state kinetic behavior of thrombin is well described by the acyl–enzyme mechanism [58]:

$$E + S \underset{k_{-1}}{\overset{k_1}{\rightleftharpoons}} E(S) \overset{k_2}{\longrightarrow} \begin{array}{c} Acyl\text{-}E \\ + \\ P_1 \end{array} \overset{k_3}{\longrightarrow} E + P_2 \tag{5}$$

Analysis of the effects of Na^+ (and other monovalent metal ions) on the individual rate constants k_1, k_{-1}, k_2 and k_3 in Eq. (5) demonstrated that all these constants are increased by Na^+ binding. These workers propose a two state model in which the binding of Na^+ acts as an allosteric effector to trigger a transition between two conformational states designated as slow and fast reacting that may correspond to "closed" and "open" forms. The dissociation constant for Na^+ binding to the native enzyme is about 20 mM ($\Delta G = -2.27$ kcal mol^{-1}) [50]. This affinity varies with the state of the enzyme; the E(S) complex has a higher affinity (-2.76 kcal mol^{-1}) as does the acyl-E (-2.41 kcal mol^{-1}). The relative rate k_2 of acylation and rate k_3 of deacylation for the amide substrate S-2238 are switched (k_2 is increased 1.5-fold, while k_3 is increased twentyfold). It is note worthy that Na^+ binding in this system changes the rate-limiting step for catalysis. This fact and the increased rates for other steps in the mechanism show that Na^+ binding not only switches the protein between two conformational states but also selectively alters the activation energies of individual steps along the reaction path.

According to the hypotheses outlined above and the two examples given, cofactor binding can selectively decrease the activation energy for a particular chemical process through selective binding to a particular enzyme conformation. Within the context of enzyme evolution, it then would seem that activation via such mechanisms represents the fine tuning of highly evolved catalysts [50]. Because Na^+ and K^+ are ubiquitous in biological milieu, there is a logic to the evolution of enzyme systems that take advantage of the presence of these metal ions as activating cofactors.

3. The coordination chemistry of Na^+ and K^-

3.1. Simple complexes

The M^+ ions derived from the group I elements have a single s electron outside a noble gas core and thus are spherical and exhibit low polarizability [77,78]. Table 1 compares some of the properties of the group I monovalent ions, from Li^+ to Cs^+. The crystal ionic radii (for six-coordination) increase from 0.74 Å (Li^+) to 1.70 Å (Cs^+), with values of 1.02 Å and 1.38 Å respectively for Na^+ and K^+. The differences in charge density due to these differences in ionic radii give rise to considerable differences in hydration behavior. These differences are indicated by the trends in hydration radii, the approximate hydration numbers and the hydration energies listed in Table 1 [78]. Neutron diffraction studies indicate that Li^+ and Na^+ are surrounded by at least six water molecules in a primary hydration sphere

Table 1
Some properties of the alkali metals and their ions[a]

	Alkali metal				
	Li	Na	K	Rb	Cs
Atomic number	3	11	19	37	55
Electronic configuration	[He] $2s^{-1}$	[Ne] $3s^{-1}$	[Ar] $4s^{-1}$	[Kr] $5s^{-1}$	[Xe] $6s^{-1}$
Atomic radius[b] (Å)	1.52	1.86	2.27	2.48	2.65
$H°$, atomization (kJ mol^{-1})	161	108	90	82	78
Melting point (°C)	180	98	64	39	29
Boiling point (°C)	1326	883	756	688	690
First ionization energy (kJ mol^{-1})	520	496	419	403	375
Second ionization energy (kJ mol^{-1})	7297	4561	3069	2650	2420
Ionic radius[c] (Å)	0.74	1.02	1.38	1.49	1.70
$H°$, hydration of M^+ (kJ mol^{-1})	−528	−413	−330	−305	−280
$S°T$, hydration of M^+ (kJ mol^{-1})	−140	−110	−70	−70	−60
$G°$, hydration of M^+ (kJ mol^{-1})	−485	−379	−308	−285	−262
$EM^+(aq)+e^-$ (M V^{-1})	−3.04	−2.71	−2.92	−2.99	−3.02

[a] Values taken from Ref. [78] with permission.
[b] In b.c.c. metal.
[c] For six-coordination.

[78]. K$^+$, Rb$^+$ and Cs$^+$ have ionic radii that are large enough to accommodate more than six water molecules in their primary hydration spheres. Both Na$^+$ and K$^+$ have been shown to form complexes containing as many as eight to ten ligands in geometries determined by the structure of the chelator. The electrostatic interactions between Na$^+$ and K$^+$ and the water molecules in the first hydration shell are not sufficient to accommodate the metal ion charge [77]; hence the residual electrostatic field causes additional water molecules to be bound in outer layers, and the strength of these interactions sharply decreases with increasing distance from the metal center. The hydrated radii given in Table 1 indicate that (as expected) the importance of additional water shells to the hydrated radii decreases as the crystal radius increases.

According to the data in Table 1, the aqueous solution coordination chemistries of Na$^+$ and K$^+$ with simple ligands are dominated by the free energies of hydration which work against the formation of complexes with chelators or, in the case of MMA enzymes, chelation sites on the protein. Hence, the strength of binding of a monovalent metal ion to a chelator or to a protein site is determined in part by two opposing forces: the attractive electrostatic forces provided by the liganding atoms, and the interaction of water molecules with the free site and the free metal ion. These effects are very different for Na$^+$ and K$^+$; the smaller ionic radius and therefore higher charge density on Na$^+$ gives this ion a hydration free energy that is 71 kJ mol^{-1} (17 kcal mol^{-1}) [78] more favorable. Since at least partial loss of the sphere of hydrating water molecules is obligatory for the formation of a protein complex, the strength of the ligand field at the metal site and the ionic radius of the metal ion can provide part of the basis for selectivity in metal ion binding to proteins. Therefore discrimination between Na$^+$ and K$^+$ that includes the effects of solvent can be built into a protein site as a consequence of evolutionary pressures [3].

3.2. Macrocyclic multidentate complexes — models for protein complexes

There exists a large general class of cyclic organic chelators known as macrocyclic multidentates (MCMs) which form host–guest complexes with group I metal ions [79–82]. Most of these compounds are based on the crown-ether-type structure and have been given names such as cryptaspherands, cryptands, spherands, hemispherands, corands and podands to indicate the number of rings, the presence of donor atoms other than oxygen and the extent to which the MCM can encapsulate the guest ion. These complexes exhibit coordination numbers typically ranging from four to ten, depending on the macrocycle structure, and the number of coordinated anions and solvent molecules. Bond lengths in these complexes are quite variable. For example, a sampling of Na$^+$—O bond lengths in crown ether complexes range from 2.26 to 3.30 Å (see Table 1 of Ref. [79]). Many of these chelators form complexes that encapsulate the cation and have found wide use as agents that solubilize these ions in non-aqueous milieu. Certain of these MCM systems form complexes with a hydrophobic exterior making them permeable to lipid bilayers and therefore able to effect the transport of Na$^+$ and K$^+$ across biological membranes with high selectivities. These systems mimic some of the properties of the naturally occurring neutral

and carboxylic antibiotic ionophores produced by fungi and bacteria. The neutral antibiotics include valinomycin, enniatin, beauvericin and the nonactin family [81,83–87]. The carboxylic acid antibiotics include monensin, nigericin, grisorixin, carriomycin, emericid, septamycin and many others [81,88,89]. The MCMs usually have core structures derived from rings of variable size that include three to ten or more neutral donor atoms (usually oxygen and nitrogen) which can coordinate the metal ion [79–82]. The MCMs with the highest affinities and selectivities contain a variety of oxygen and nitrogen donor atoms appropriately located in rigid bicyclic, tricyclic and multicyclic ring systems [82]. In these MCM complexes, the bond lengths between the donor atom and the metal ion depend on the number, size and charge density of the donor atoms and on bonding constraints imposed by the structure of the MCM. Shannon [90] has published a set of effective ionic radii for monovalent, divalent and trivalent metal ions that reflect the effects of coordination number. Data taken from Shannon [90] showing the dependence of effective ionic radii on coordination number for monovalent cations are presented in Fig. 3.

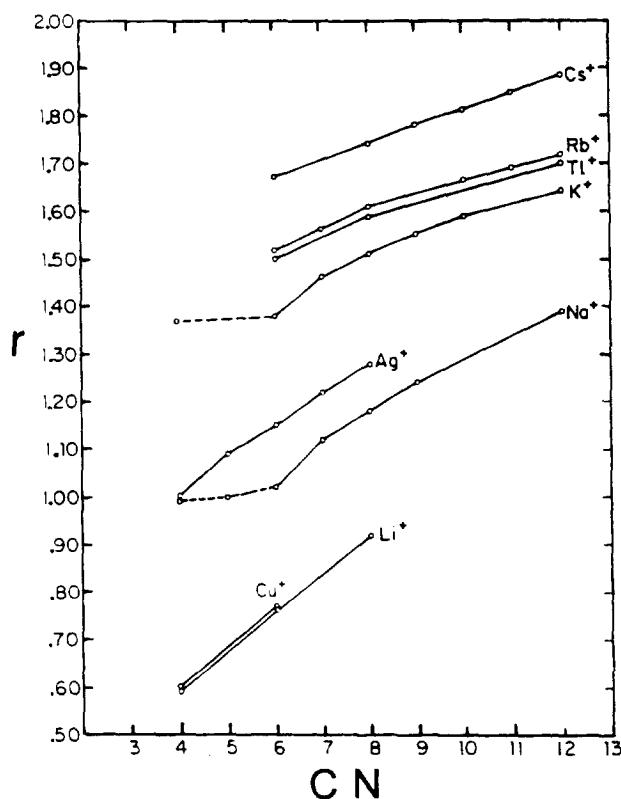The neutral ionophores such as valinomycin, enniatin and beauvericin are cyclic

Fig. 3. Plot of effective ionic radii (in ångströms) vs. coordination number (CN) for group I metal ions. (Taken from Ref. [90] with permission.)

polydepsipeptides usually with a repeating sequence of two or four units (α-amino acids and α-hydroxy acids) which sometimes are chemically modified [81]. The nonactin family have macrocyclic polyester structures built up of four nonactic acid derivatives of alternating chirality [81]. The valinomycin-type ionophores form complexes in which six ester carbonyl oxygen atoms are the donor atoms to the metal ion [81]. The cyclic encapsulate-like structure is stabilized by six hydrogen bonds involving the ring amide linkages to give a ribbon of β structure around the periphery of the complex. Valinomycin shows one of the highest selectivities, favoring K^+ over Na^+. Nonactin also shows a high degree of selectivity for K^+ in comparison to Na^+ [81]. Structures of nonactin and the nonactin Na^+ and K^+ complexes are shown in Fig. 4 [81,83–86]. As is evident from this comparison, the crystal structure of free nonactin is considerably different from that of the Na^+ and K^+ complexes. Uncomplexed nonactin has a somewhat flattened structure in which the donor carbonyl and tetrahydrofuran ether oxygen atoms point outward [81,83–86]. Upon complexation with either K^+ or Na^+, the molecule undergoes a large change in conformation such that the donor atoms are oriented inward toward the metal ion [81,83–86]. In the Na^+ and K^+ structures, the metal ion is positioned at the center of a nearly symmetric cubic ligand field formed by four carbonyl ester and four tetrahydrofuran oxygen donors. To accomplish the switch in orientation of the donor atoms, the 32-membered macrocycle ring is twisted into a shape that is reminiscent of the seam on a tennis ball with the metal ion located at the center of the ball [81]. This conformation places the CH_2 groups of the tetrahydrofuran rings on the perimeter of the structure, giving the complex a hydrophobic exterior. Close inspection of these structures reveals that the $K^+ - O$ bond distances are very near those expected for a coordination number of eight, with the ether oxygen bonds (mean, 2.85 Å) slightly longer than the carbonyl oxygen bonds (2.77 Å). However, there are two distinct classes of $Na^+ - O$ bond distances; the ether oxygen bonds (mean, 2.77 Å) are longer than expected, while the carbonyl oxygen bonds (mean, 2.42 Å) are nearly exactly the length expected for a cubic ligand field (Fig. 3) [90]. If all eight $Na^+ - O$ bonds were brought to the distance expected for an eight-coordinated (cubic) complex (2.40 Å), then there would be significant van der Waals conflicts between non-bonded atoms [81]. These results indicate that the nonactin macrocycle is well designed to accommodate K^+, but the nonactin cavity is unable to adjust completely to the smaller size of Na^-, and therefore the cubic coordination sphere is distorted. This compromise appears to account for the specificity of nonactin for K^+ and the weaker affinity for Na^+ [81].

Most of the carboxylic antibiotic ionophores are produced by strains of streptomyces [81]. Fungi and bacteria also produce members of this family. Studies of the structures of these ionophores by X-ray crystallography and other spectroscopic methods [81] show two types of metal ion complex: those where the terminal carboxylate is coordinated to the metal ion, and those where the terminal carboxyl group forms hydrogen-bonding interactions with other atoms of the chelator but does not coordinate to the metal ion. Those complexes in which the carboxylate is coordinated to the metal ion give structures that are in some ways similar to the metal sites in tryptophanase [9,10], TPL [6–8] and DGD [4,5]. The complexes
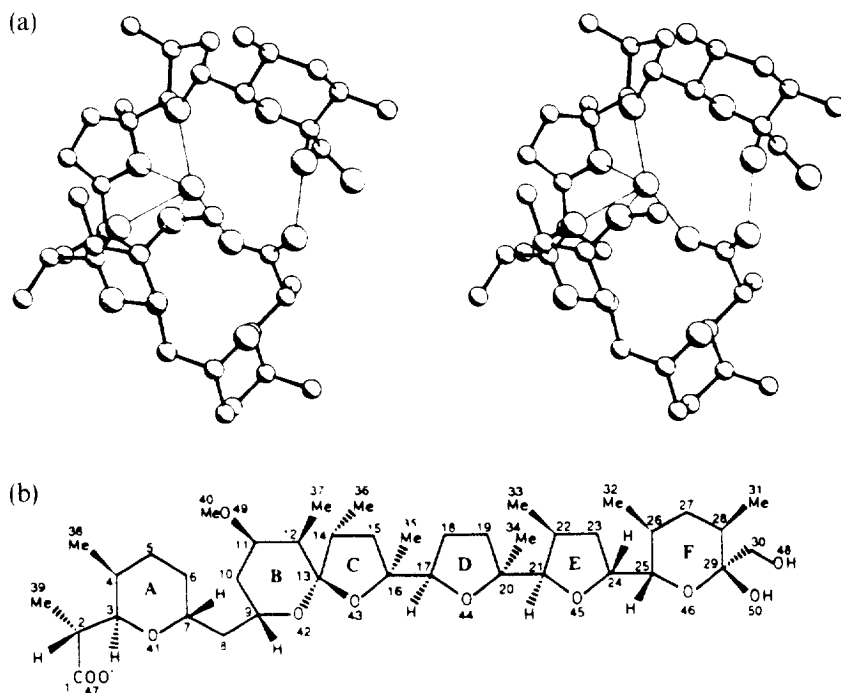
(a)

(b)

(c)

(d)

(e)

(a)

(b)
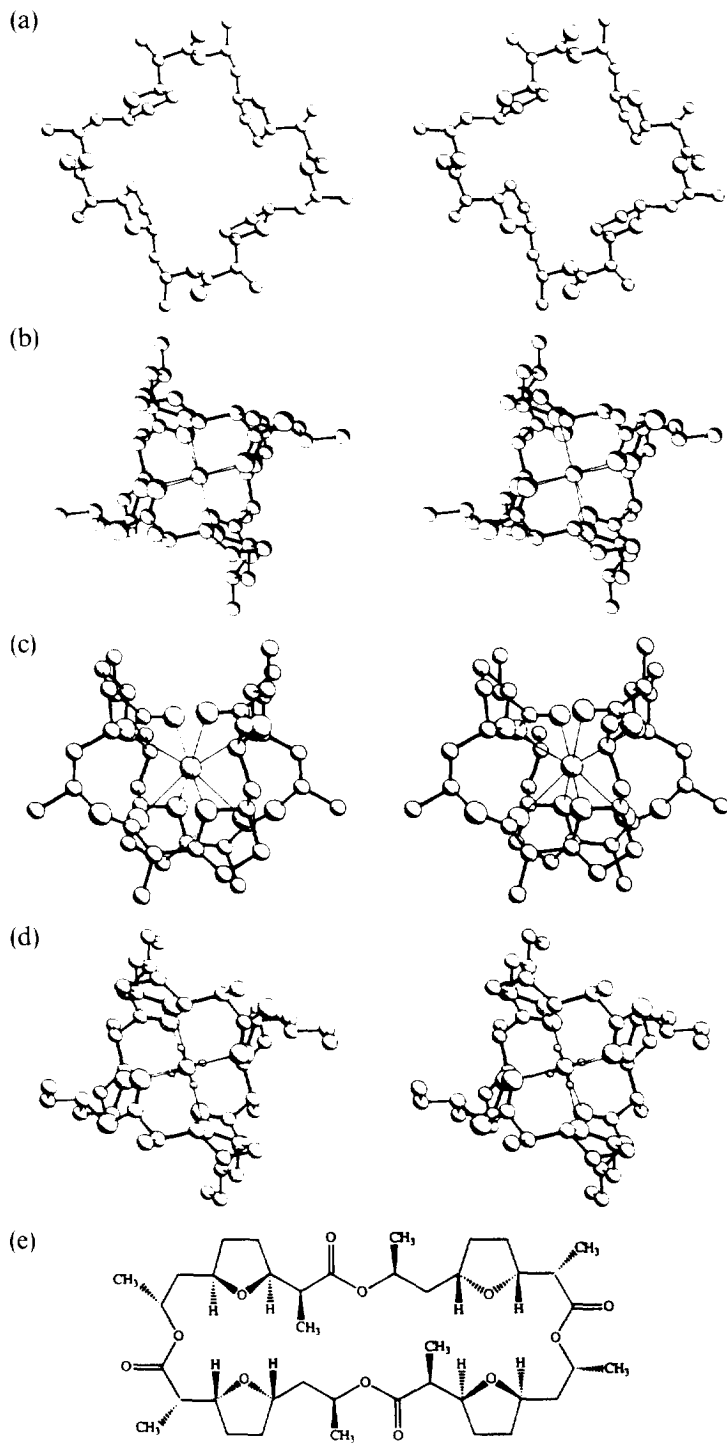
Fig. 5. (a) Stereo drawing of the X-ray structure of the nigericin–Ag⁺ complex. (Taken from Ref. [81] with permission.) (b) Schematic diagram of uncomplexed nigericin. (Taken from Ref. [89] with permission.)

formed with nigericin are typical of these structures [81,87–89] (Fig. 5(a)). The molecule (Fig. 5(b)) has a polyether structure containing three six-membered cyclic ether rings (A, B and F) and three five-membered cyclic ether rings (C, D and E). There is a spiro junction between rings B and C. One end of the molecule has a carboxylic acid group; the other has two hydroxyl groups. In both structures of the metal-free species (not shown) and the metal ion complexes (Fig. 5(a)), the carboxyl group forms hydrogen-bonding interactions with the hydroxyl groups to give a closed macroring structure with a cavity capable of binding monovalent cations [81,88,89]. As shown in Fig. 5(a), the Ag⁺ complex of nigericin involves the coordination of five donor oxygen atoms, three ring ether oxygen atoms, one methoxy oxygen atom and one carboxylate oxygen atom, in a rather irregular coordination polyhedron. The carboxylate group also makes a hydrogen bond to the hydroxyl group at the far end of the molecule in this macrocyclic structure. It has been reported that the Na⁺ and K⁺ complexes give structures that are highly similar to that of the

Fig. 4. Stereo drawings of the X-ray structures of nonactin and its monovalent cation complexes: (a) uncomplexed nonactin; (b) the Na⁺ complex; (c) the K⁺ complex; (d) the NH₄⁺ complex. (Taken from Ref. [81] with permission.) (e) A schematic diagram of the uncomplexed nonactin. (Taken from Ref. [87] with permission.)

Ag^+ complex [88,89]. In the Na^+ complex, the carboxylate oxygen bond to Na^+ is reported to be 2.24 Å, while the other $Na^+ - O$ bonds are somewhat longer (2.39–2.52 Å). The shorter bond to the carboxylate oxygen atom is expected on electrostatic grounds. As will be shown, the nigericin complexes have some similarity with the structures of the metal sites in certain PLP enzymes.

Structures of some highly selective synthetic MCM hosts and their host–guest complexes of Na^+ and K^+ designed and synthesized by Cram's group [82,91–97] are presented in Fig. 6. In these spherand and cryptahemispherand complexes [82,91,93], the bond distances are those expected for Na^+- and K^+-dipole bonds to neutral oxygen and nitrogen atoms. Comparison of the structures of the free chelators with the metal ion complexes show that the cavity of the free chelator has a conformation that is "pre-organized" to match exactly the radius of the metal ion that it was designed to bind. Accordingly, cryptahemispherand 2 (Fig. 6(b)) has a cavity that is tailored to fit the dimensions of Na^+, while cryptahemispherand 3 (Fig. 6(c)) is tailored to fit the dimensions of K^+, and cryptahemispherand 4 is tailored to fit Cs^+ (Fig. 6(f)). This complementarity conveys both high specificity and high affinity for the matching cation. The X-ray structures of the complexes with mismatched ions, e.g. the Na^+ and K^+ complexes of cryptahemispherand 4 (Figs. 6(d) and 6(e)), show that, when the ion is too small, the cavity is unable to contract sufficiently to bring each of the donor atoms into the standard bonding distance [93]. Hence, the Na^+ complex gives a distorted complex where the $Na^+ - O$ bonds to five of the donor oxygen atoms are nearly standard (2.53–2.69 Å), while the other two are longer than expected (2.78 Å and 2.85 Å) [90,93].

As shown in Figs. 4–6, the coordination of MCMs such as the antibiotic ionophores, crown ethers, cryptands and spherands to group I monovalent metal ions occurs to give encapsulates where the metal ion can be completely enveloped by the MCM. The structures of these complexes are controlled by a number of factors that reflect the properties of the metal ion (size and hardness), the available anion(s) and the structure of the MCM [79–82,91–97]. Encapsulation can bring about charge separation between the metal ion and the anion that provides charge neutralization [79,82]. Formation of a charge-separated encapsulate therefore depends on the metal ion charge density, the energy required to drive the MCM to the conformation required for wrap-around encapsulation, the strength of the dipole interaction provided by the donor atoms and the strength of the charge–charge interactions between the metal ion and the anion [79,82]. Thus the lower charge densities of K^+, Rb^+ or Cs^+ in comparison with Na^+ favor formation of charge-separated encapsulation complexes, while the higher charge density of Na^+ favors formation of anion-paired species [79].

Fig. 6. Schematic diagrams and stereo drawings of the spherand and cryptahemispherand complexes of various group I metal ions. (a) spherand 1 and its complex with Li^+. (Taken from Ref. [91] with permission.) (b) The Na^+ complex with cryptahemispherand 2. (c) The K^+ complex with cryptahemispherand 3. (d) The Na^+ complex with cryptahemispherand 4. (e) The K^+ complex with cryptahemispherand 4. (f) The Cs^+ complex with cryptahemispherand 4. (Taken from Ref. [93] with permission.)

(a) 1

Na⁺ - 2 (b)

K⁺ - 3 (c)

Na⁺ - 4 (d)

K⁺ - 4 (e)

Cs⁺ - 4 (f)
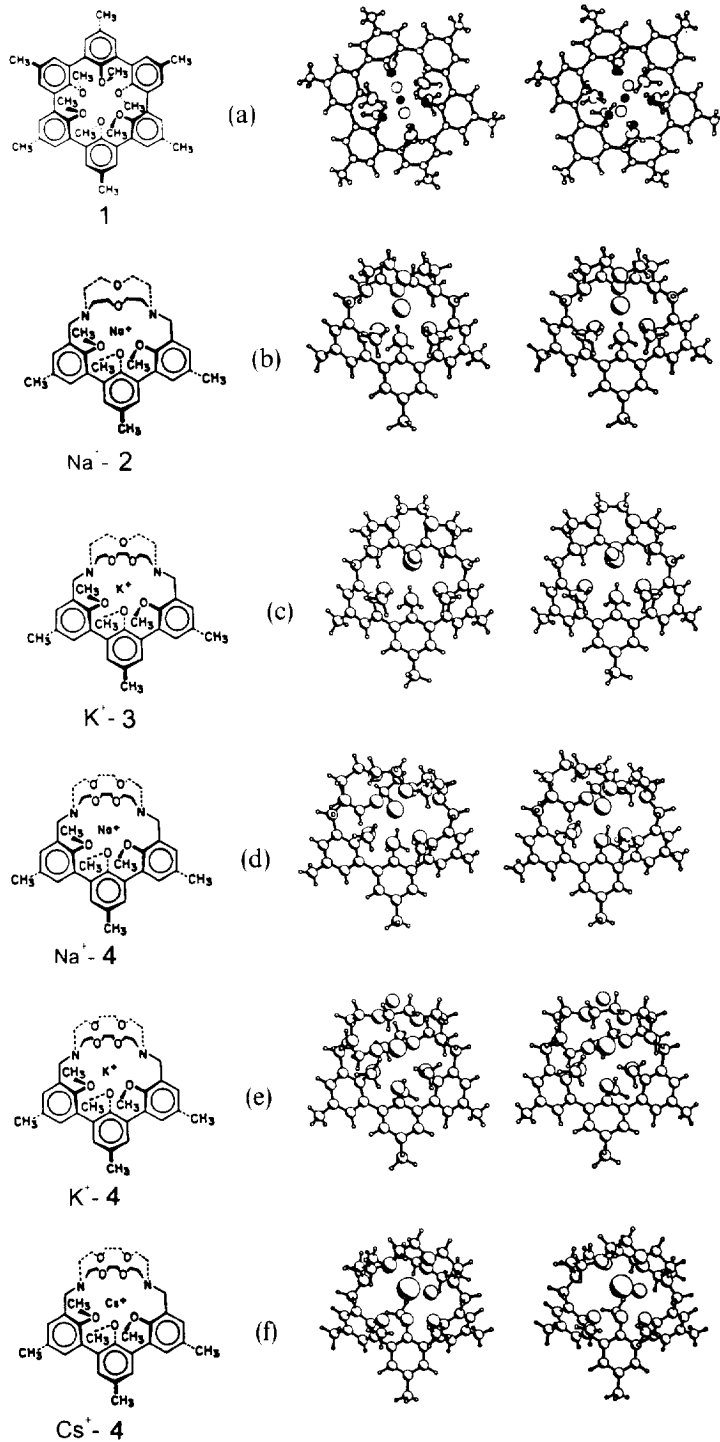
3.3. Specificity in macrocyclic multidentate encapsulation

Until recently, no single unifying set of principles was available to explain the selectivities exhibited by various MCMs for individual ions of the group I series [79]. Since the structures of the MCMs are quite varied with respect to the rigidity, the cavity size, the number of donor atoms and the ability to encapsulate, it is not surprising that it has been difficult to perceive the unifying principles which govern selectivity. The elegant work of Cram's group [82,91–97] has conclusively shown that the matching of the host cavity to the size of the guest metal ion is a factor of considerable importance. This factor and pre-organization of a rigid host cavity (via synthesis) are of overriding importance for conveying both high affinity and high selectivity to the interaction between host and guest [82]. Pre-organization mini-mizes unfavorable changes in the internal degrees of freedom of the host resulting from complexation. Furthermore, pre-organization of the host may introduce repul-sions between the non-bonded electron pairs of the donor atoms at the site that are relieved when the metal ion binds [82,91–98]. Because of steric constraints, such an arrangement of the donor atoms may reduce or eliminate altogether the solvation of the site prior to complexation. Guest cations which do not match the dimensions of a rigid host cavity will exhibit a decreased affinity because the poor fit may cause the host to present an asymmetric set of bonding interactions that therefore do not match the spherical distribution of charge on the metal ion [82]. To satisfy charge dipole requirements, the poorly fitting metal ion may form a distorted host–guest complex with a less favorable conformation involving strained bond lengths and angles [82,83,91–95].

Selectivity therefore depends on a variety of factors including cooperative inter-actions between the MCM and the metal ion that compete favorably with solvent and with other cations of differing size and hardness. As exemplified in Fig. 6, Cram et al. [91] have been successful in designing host spherands and cryptahemispherands which highly selectively encapsulate each of the group I metal ions and bind with high affinity. These MCMs are composed of sterically and covalently formed rigid cavities lined with the unshared electron pairs of the donor atoms. The key to the preparation of highly selective high affinity MCMs is the synthesis of rigid com-pounds that are constrained by covalent bonding and non-bonding interactions that almost perfectly pre-align the unshared electron pairs in a cavity with dimensions that match the optimum bond lengths of the metal ion for which the MCM is designed. These empty cavities are surrounded by a hydrocarbon shell of alkyl and/or aryl groups. Hence the liganding atoms are deeply buried away from the solvent, and complexation requires little or no reorganization of the solvent about the host. The selectivity of some of these systems is so high that they can be used to scavenge Na^+ or Li^+ from bulk solutions of K^+, Mg^{2+} or Ca^{2+} [82,91]. The most specific hosts for Li^+ and Na^+ have nearly ideal cavities for matching these cations. This match involves the aligning of donor group dipoles directly toward the cation on the inner surface of a cavity that matches the diameter of the metal ion. The spherand with the structure in Fig. 6(a) is estimated to bind Na^+ more tightly than K^+ by about 40 kcal mol^{-1} (ΔE) [91]. The importance of these factors to the design of

effective MCMs is illustrated by the fact that the intrinsically poor anisyl oxygen donor, when pre-organized into the spherand shown in Fig. 6(a), becomes an extremely effective and highly discriminatory chelator for Li^+ and Na^+ but has negligible affinity for K^+ and larger monovalent metal ions.

In summary, high selectivity and high affinity can be achieved by the design of MCMs with the following characteristics: (1) the MCM must have a rigid pre-organized structure, (2) the rigid structure must form a cavity with nearly perfect dimensions tailored to the size of the metal ion, (3) this rigid cavity should provide a set of donor atoms with nearly perfectly aligned dipoles and appropriately located unshared electron pairs to satisfy the bonding needs and electrostatic requirements of the metal ion and (4) the cavity must be shielded from solvent by a low dielectric (hydrocarbon) outer skin. When these design criteria are met, highly selective chelators with high affinities can be made [82].

3.4. Protein complexation of group I metal ions

As will be seen below, because the in-vivo free concentrations of Na^+ and K^+ can be in the 20–50 mM range, protein sites for these metal ions need only be able to compete with the aqueous environment. Sites with dissociation constants in the 0.1–10 mM range have sufficient affinity to ensure occupation by Na^+ or K^+ under most physiological conditions. Achievement of high affinities in the MCM systems described above requires complete pre-organization and low solvation of a rigid host cavity prior to metal ion binding. However, the biological functioning of a monovalent metal ion site almost certainly is dependent upon a certain degree of flexibility of the protein matrix that comprises the metal site so that bonding interactions at the metal site can be communicated to the catalytic site (see the enzyme examples discussed in Section 5 and Eqs. (1)–(4)). The result necessarily will be a sacrifice of selectivity and affinity for the conformational flexibility necessary for biological function.

Because there are large intracellular and extracellular differences in the concentrations of Na^+ and K^+, it appears that, as a general rule, metal ion specificity is configured such that enzymes which reside within the cell where the concentration of K^+ is greater than Na^+ exhibit specificity for K^+. Extracellular enzymes which reside in milieu where the concentration of Na^+ usually is greater than K^+ exhibit specificity for Na^+.

4. Structure–function relationships in pyridoxal phosphate-requiring enzymes

4.1. General considerations

Christen's group [99] has investigated the evolutionary relationships among PLP-requiring enzymes using computer-assisted algorithms for comparison of amino acid sequences. These analyses, involving nearly 300 sequences of about 50 enzymes, establish that PLP enzymes have multiple evolutionary origins and that there are

several families of homologous proteins. Three main enzyme families were identified which process amino acids, and these have been designated as the α, β and γ families with reference to the amino acid carbon loci of the bond scission–bond formation reactions catalyzed by each family. Hence, with few exceptions, the α-family members catalyze bonding changes at the substrate amino acid α-carbon, while the β- and γ-family members catalyze reactions at the β- and γ-carbons of their respective substrates. Christen and co-workers [99] have proposed that the progenitor PLP-dependent enzymes were regiospecific catalysts and that reaction specificity (i.e. specificity for the carbon locus) preceded specificity for substrate shape. Furthermore, PLP-requiring enzymes do not seem to be related to any non-PLP-requiring enzymes of known sequence; consequently, this class of enzymes may have developed at a very early stage of evolution.

Of importance to this review is the observation that DGD, tryptophanase and TPL all belong to the α family (which also includes most aminotransferases, decarboxylases, acyltransferases, some racemases and various other miscellaneous PLP enzymes) [99]. While DGD carries out reactions (decarboxylation and transamination) that are restricted to the α-carbon atom of its amino acid substrates, tryptophanase and TPL are exceptions to the rule in that these enzymes carry out cleavages that involve the β-carbon atoms of their respective substrates. Nevertheless, these three enzymes share many of the same folding motifs [4–10] (see below), and this similarity extends to the level of the location and structure of the active sites. In all three enzymes the catalytic sites include contributions from residues contributed by the crystallographically related subunit. However, unlike TPL and tryptophanase, where the metal sites include ligands from the adjacent subunit, the ligands to the DGD K^+ site are all derived from the same subunit. In view of these structural similarities, it seems likely that many of the other enzymes in this family will turn out to be activated by monovalent metal ions.

The β family is comprised of PLP enzymes that catalyze β replacement and β elimination reactions, and includes such enzymes as L- and D-serine dehydratases, threonine dehydratase, tryptophan synthase (β-subunit) threonine synthase and cysteine synthase. The folding motif which characterizes this family is very different from that of the α family; therefore it seems unlikely that these two families originated from a common ancestral protein [99]. Within this family, it is known that tryptophan synthase is subject to activation by certain group I metal ions.

The γ family is relatively small and includes PLP enzymes that catalyze γ replacement and γ elimination reactions such as O-succinylhomoserine (thiol)-lyase, O-acetylhomoserine (thiol)-lyase and cystathionine γ-lyase. One exception, which catalyzes a β-carbon reaction, has thus far been identified: cystathionine β-lyase.

4.2. Principles of catalysis and reaction specificity in pyridoxal phosphate enzyme catalysis

PLP-requiring enzymes are involved in an amazing variety of chemical transformations, many of which are of central importance to nitrogen metabolism in all

organisms. The bio-organic chemistry and enzymology of PLP enzyme catalysis has been reviewed in depth [100–111] and is given considerable space in most biochemistry textbooks. Therefore this review will only treat those aspects of PLP enzyme reaction mechanism that are directly pertinent to the subject of monovalent cation activation. Simply stated, these are as follows:

(1) PLP enzymes that catalyze transformations of amino acids initiate reaction via formation of a Schiff base (external aldimine) intermediate formed between the α-amino group of the substrate and the C(4') carbon atom of enzyme-bound PLP. Protonation of the PLP pyridine ring nitrogen atom and the Schiff base imine nitrogen atom create an electron "sink" effect that can facilitate heterolytic cleavage of any of the three bonds to the Schiff base α-carbon atom. The resulting carbanion is a highly resonance-delocalized species that is often represented by a quinonoidal canonical structure. Formation of a quinonoidal intermediate is obligatory for all PLP enzymes involved in amino acid metabolism.

(2) In order for facile cleavage of one of the three bonds to the α-carbon atom to occur, the σ bond cleaved must be oriented with respect to the PLP π system such that orbital overlap between the nascent π orbital (in which the carbanion electron pair formally resides) is maximized [109,110]. The energy barriers to cleavage of bonds oriented orthogonal to the π system is prohibitively high. This bond cleavage imperative provides the basis for stereospecificity and regiospecificity [109,110] (Dunathan's hypothesis). The rotomer conformation of the bound external aldimine is controlled via weak bonding interactions involving the α-carboxylate group and/or the side-chain group of the reacting substrate and specificity subsites on the protein for these groups.

(3) Consequently, if the enzyme site dictates the orientation of the amino acid moiety relative to the disposition of the PLP ring π system (through weak bonding interactions), then the site will be selective both for a particular α-carbon stereo isomer and for the particular α-carbon bond to be cleaved [109,110]. As a corollary, PLP enzymes which catalyze bond changes at the β- and γ-carbon atoms must meet similar orbital alignment criteria for catalysis.

These bio-organic mechanistic considerations imply that one possible mechanism for the involvement of monovalent metal ions as allosteric effectors of PLP enzymes could involve metal-ion-mediated conformational transitions which drive an enzyme-bound intermediate to a structure where the bond to be cleaved (or formed) has optimal alignment with the PLP ring π system.

4.3. Monovalent metal ion activation of tryptophanase

4.3.1. Background

Tryptophan indole-lyases (tryptophanases) are found in enteric bacteria, molds, yeasts and plants [100,104,106,108]. These enzymes catalyze scission of the C—C bond between the indole ring and the β-carbon atom of L-tryptophan to yield indole, ammonia and pyruvate via a β-elimination and deamination:

$$\text{L-Trp} \quad + \quad \text{H}_2\text{O} \quad \overset{\text{Tryptophanase}}{\rightleftharpoons} \quad \text{Indole} \quad + \quad \text{Pyruvate} \quad + \quad \text{NH}_4{}^+ \tag{6}$$

The catalytic mechanism for this transformation involves the conversion of the internal aldimine form of the enzyme through the series of discrete covalent intermediates shown in Scheme 1 [106,112].

It has been known for many years [19,20,22,106,113–115] that tryptophanase is activated by certain monovalent cations ($\text{NH}_4^+ > \text{K}^+ > \text{Cs}^+ > \text{Na}^+ > \text{Li}^+$). Morino and Snell [19,20] and Suelter and Snell [22] showed that the native enzyme exists in two interconvertible pH-dependent forms of the internal aldimine, E(Ain) (Scheme 1), with PLP absorption bands at 337 and 420 nm. At pH 7.2, K^+ binding drives the distribution of forms in favor of the 337 nm species, while Na^+ stabilizes the 420 nm species [19,22]. Metzler et al. [24] have very nicely exploited the different effects of Na^+ and K^+ on tryptophanase as a means for preparing apo (PLP-free) enzyme. They found that potassium phosphate stabilizes the holoenzyme but that dialysis against sodium phosphate buffer in the presence of L-Ala achieves a rapid and quantitative release of PLP. Furthermore, in the presence of K^+ the enzyme reacts with a variety of amino acid substrates and substrate analogues to give quinonoidal species E(Q) with intense absorption maxima in the vicinity of 500 nm (Fig. 7), while virtually no quinonoidal species are detectable when K^+ is substituted by Na^+ [22]. Suelter and Snell [22] found that metal ion binding perturbs the enzyme spectrum and these perturbations could be used to estimate the dissociation constants for monovalent cation binding. Comparison of these values with K_m and V_{max} values for the tryptophanase-catalyzed elimination of o-nitrophenol from S-o-nitrophenyl-L-Cys (SOPC) [22] gave the results shown in Table 2.

These data show that NH_4^+ is the most effective cation in this series for activating the elimination reaction with SOPC; NH_4^+ has the highest affinity for the enzyme and gives the lowest K_m and highest V_{max} values for the substrate. While Na^+ brings about significant activation of the enzyme, the finding that quinonoidal species are not formed in appreciable amounts with this cation strongly indicates that K^+ gives highly selective interactions with certain covalent intermediates along the reaction path that are different from those with Na^+. These interactions selectively alter the ground-state stabilities of some species relative to others and lower the activation energies for certain steps. It is particularly clear that K^+ binding greatly stabilizes the ground state of the quinonoidal species and lowers the activation energy for the conversion of the external aldimine Schiff base, E(Aex1) (Scheme 1), to the quinonoid, a process which involves the abstraction of the α-proton of the aldimine by a base at the enzyme site.

4.3.2. Structural details of the K^+ site in tryptophanase

Fig. 8 presents a ribbon cartoon of the tryptophanase dimeric unit showing the subunit folding motif, the monomer–monomer interface and the location of the K^+ sites as viewed along the molecular twofold axis of symmetry [9]. Fig. 9 is a stereo drawing showing the geometry and bonding details of the K^+ site. This site was
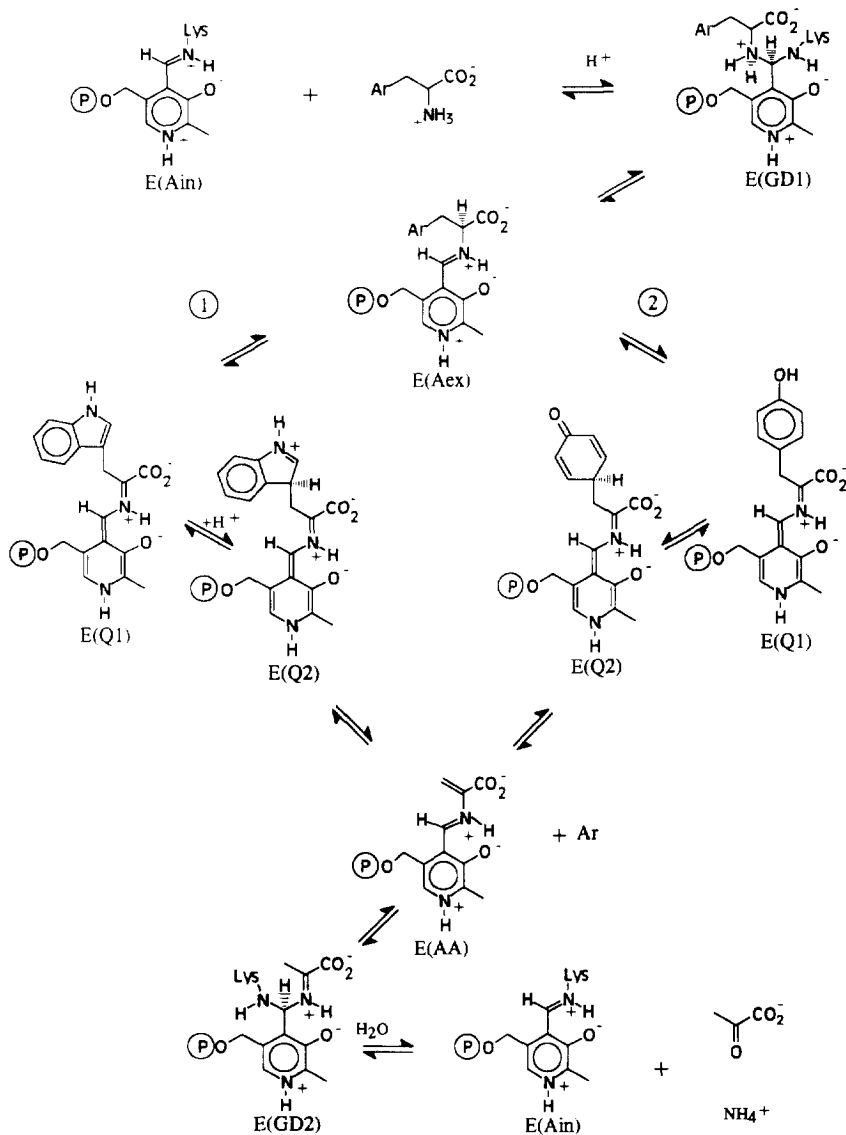
Scheme 1. Outline of the steps for the reactions catalyzed by tryptophanase (pathway 1) and TPL (pathway 2), showing organic structures of the chemical intermediates. For pathway 1, Ar- is the indole moiety; for pathway 2, Ar- is the phenol moiety. The structure designations for PLP species are as follows: E(Ain), internal aldimine Schiff base; E(GD1) and E(GD2), the first and second gem-diamine intermediates respectively; E(Aex), the amino acid substrate external aldimine Schiff base; E(Q1) and E(Q2), the first and second quinonoidal species respectively; E(AA), the α-aminoacrylate Schiff base.
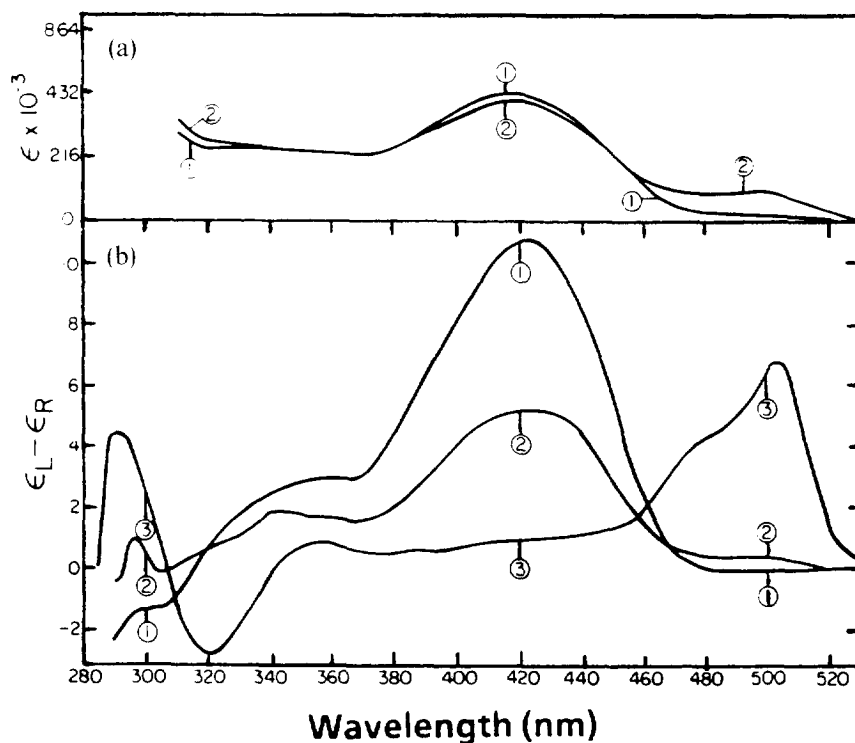
Wavelength (nm)

Fig. 7. (a) Absorption spectra of holotryptophanase (2.5 mg ml^{-1}) in 0.025 M (CH$_3$)$_4$N–Hepps at pH 8.0 and room temperature: spectrum 1, holotryptophanase; spectrum 2, holotryptophanase plus 10 mM ethionine. (b) circular dichroic spectra of holotryptophanase (3.2 mg ml^{-1}): spectrum 1, holotryptophanase; spectrum 2, holotryptophanase plus 10 mM ethionine; spectrum 3, holotryptophanase plus 10 mM ethionine and 0.1 M KCl. (Taken from Ref. [22] with permission.)

Table 2
Steady state kinetic parameters for the activation of tryptophanase cleavage of S-o-nitrophenyl-L-Cys[a]

M$^+$	K_a (mM)	K_m (mM)	v_{max} (μmol min mg^{-1})
Li$^+$	54 ± 11.6	0.068 ± 0.007	4.3 ± 0.28
Na$^+$	40 ± 0.06	0.245 ± 0.03	18.8 ± 1.0
K$^+$	1.44 ± 0.06	0.071 ± 0.007	35.6 ± 2.1
Cs$^+$	14.6 ± 2.6	0.155 ± 0.027	21 ± 2.3
NH$_4^+$	0.23 ± 0.01	0.055 ± 0.005	57.9 ± 2.6

[a] Values taken from Ref. [22] with permission.

identified in the refined model on the basis of the temperature factors, the coordination distances and the sequence homology with the tyrosine-phenol lyase site (see below) [10]. The ligand field consists of the backbone carbonyl oxygen atoms of

Fig. 8. Stereo ribbon cartoon showing the folding of the tryptophanase dimeric unit. The locations of the K$^+$ sites at the monomer–monomer interface are indicated by circles. The locations of the C and N termini are also indicated. (Drawing provided courtesy of M.N. Isupov.)
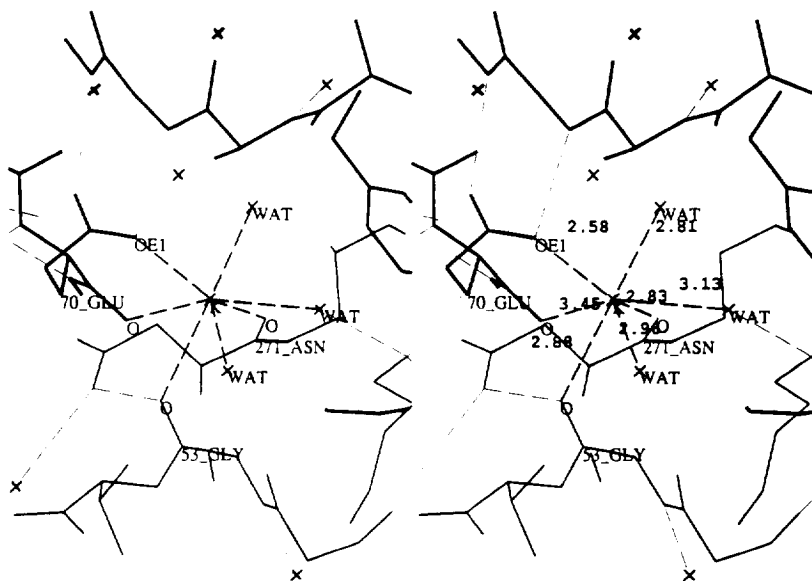

Fig. 9. Stereo drawing showing details of the K$^+$ site in tryptophanase. (Drawing provided courtesy of M.N. Isupov.)

Gly53, Glu70 (from the adjacent subunit) and Asn271, one side-chain carboxylate oxygen atom of Glu70 and three water molecules. As expected from electrostatic considerations, the shortest bond is to the carboxylate oxygen atom of Glu70 (2.58 ± 0.2 Å); the bonds to Gly53 and Asn271 are typical of K$^+$—O bonds to carbonyl oxygen (with lengths of 2.88 ± 0.2 Å and 2.83 ± 0.2 Å respectively), as are

the bonds to water (2.81, 2.96 and 3.13 ± 0.2 Å). The metal ion is located near the surface of the protein, it forms part of the subunit interface and, via the three water molecules, is exposed to solvent on one face of the coordination polyhedron. This metal site is located about 15–18 Å from the closest PLP ring and lies outside the confines of the catalytic site.

4.4. Monovalent metal ion activation of tyrosine phenol-lyase

4.4.1. Background

TPL is a close structural homologue of tryptophanase [99], and this enzyme carries out a mechanistically very similar reaction, the cleavage of L-Tyr to give phenol, ammonium ion and pyruvate [106,116] (Scheme 1):

$$\text{L-Tyr} \quad + \quad \text{H}_2\text{O} \quad \xrightleftharpoons{\text{TPL}} \quad \text{Phenol} \quad + \quad \text{Pyruvate} \quad + \quad \text{NH}_4{}^+ \tag{7}$$

The studies of Chen and Phillips [27] and Kiick and Phillips [116] on TPL and work on tryptophanase [19–26,52–56,112], have shown that these enzymes have catalytic mechanisms which (although differing in some interesting details [112,116]) overall are quite similar (Scheme 1), a finding that is in agreement with the close structural homology [6–10]. The effects of K^+ on the catalytic activity of TPL are quite similar to those described above for tryptophanase [27]. The formation of quinonoidal species E(Q) derived from L-amino acid analogues of L-Tyr, e.g. from L-Ala, requires K^+ [27,117]. However, D-Ala forms a quasi-stable quinonoidal species in the absence of metal ions; addition of K^+ (up to 10 mM) shifts the distribution of species formed with D-Ala in favor of the quinonoid species [27]. Above 10 mM, there is a further redistribution that decreases the amount of quinonoidal species. These observations indicate that the quinonoids formed from D- and L-Ala are structurally different (in agreement with Dunathan's hypothesis) [109,110], that the influence of K^+ on the ability of the protein to stabilize these two quinonoids is different, and that there may be more than one K^+ binding site per subunit on the protein.

4.5. Structural overviews of tyrosine phenol-lyase and tryptophanase

The three-dimensional structure of TPL from *Citrobacter freundii* has been reported at 2.3 Å resolution (R factor, 16.2%) by Antson et al. [8]. Like tryptophanase, TPL is a homotetramer with dimensions of approximately $80 \text{ Å} \times 60 \text{ Å} \times 105 \text{ Å}$. A cartoon showing the arrangement of subunit domains and subunit interfaces is presented in Fig. 10 [8]. The subunit arrangement is that of a dimer of dimers (with overall symmetry of 222) wherein symmetry-related monomers form a dimer and two dimers arranged about a molecular twofold axis generate the tetramer. Hence, there are two classes of subunit interfaces: interactions across the monomer–monomer interface, and interactions across the dimer–dimer interface.
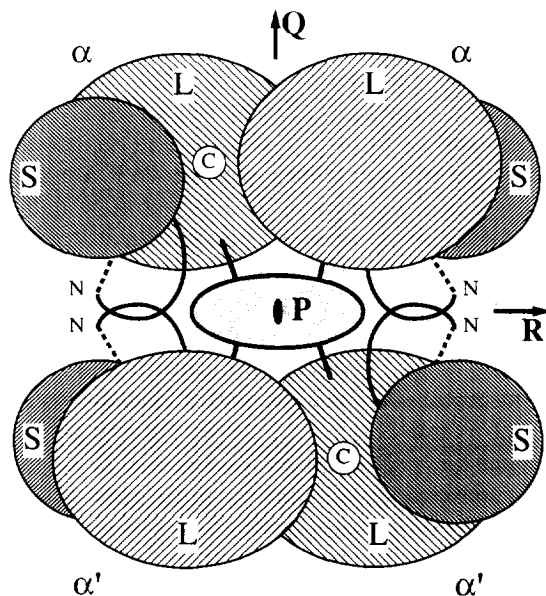
Fig. 10. Schematic representation of the domain architecture and intersubunit contacts in TPL viewed with the crystallographic twofold axis (Q) vertical and the non-crystallographic axes (P and R) horizontal. Pairs of crystallographically related subunits are labeled α and α'. Large domains are labeled L and small domains S, the catalytic cleft is labeled C, and the N termini are labelled as N. (Taken from Ref. [8] with permission.)

Dimeric units of TPL [6–8] interact through an antiparallel β sheet structure comprised of the N-terminal residues 1–18 from each of the subunits. This contact is stabilized by additional β strands. An additional set of interactions involving four Met residues and one Trp residue from each subunit combine in a hydrophobic cluster at the center of the tetramer. Each subunit is made up of two domains, one large and the other small (Fig. 10). The small domain consists of 34% of the total and includes residues from the N-terminal (19–48) and C-terminal (333–456) regions of the sequence. The folding motifs consist of a four-stranded antiparallel β sheet core from the C-terminal portion and four α helices from the N-terminal portion arranged on the solvent accessible side of the sheet. A parallel β bridge connects the two portions of this domain. The large domain (residues 57–310) makes up 56% of the total, and it also has a β sheet core (seven strands) flanked on one side with nine α helices that shield the solvent-accessible face of the β sheet. Two additional helices are positioned on the opposite face and form part of the interface between domains.

The folding of the dimeric unit is very similar to that of aspartate aminotransferase (AspAT) even though there is no significant sequence homology. This similarity extends to the arrangement of the active sites [6–8]. The catalytic site is formed by a crevice between the large and small domains and involves residues Thr49, Asp50, Ser51 and Gly52 from the connecting region, Gln98, Gly99, Arg100, Asn185, Asp214, Ala215, Thr216, Arg217, Ser254, Gly255, Lys256 and Lys257 from the large domain

and His343 and Arg404 from the small domain [8]. The site structure is completed by residues Tyr71 and Glu286 from the large subunit of the adjacent monomer. Lys257 is the active site residue which forms a Schiff base with the C(4') atom of PLP in the native enzyme structure [8]. The AspAT catalytic site also involves a similar complement of residues from each domain and contributions from the adjacent subunit. Most of the residues which contact PLP are conserved in the two enzymes. The involvement of residues from both subunits indicate that the dimer structure is essential for catalysis, whereas the tetrameric structure of TPL and the dimeric structure of AspAT imply that the tetrameric structure may not be essential for TPL.

4.5.1. Structural details of the K^+ site in tyrosine-phenol lyase

The structure of the metal site [6–8] is nearly identical with the tryptophanase K^+ site (compare Figs. 9 and 11). Fig. 11 shows the complex formed when K^+ is replaced by the heavier Cs^+. This site is identified as a K^+ site on the basis of electron density difference maps calculated from Cs^+ and K^+ data. The difference maps gave clear high peaks which are ascribed to the cation sites [7]. This structure is currently at 2.5 Å resolution. The protein residues providing the donor ligands are conserved. Like the active site, the monovalent cation binding site (Fig. 11) involves donor atoms derived from residues located in both subunits of the dimeric unit [6–8]. The four donor atoms from the protein are the main chain carbonyl oxygen atoms of Gly52 (part of the connecting bridge between domains) and Asn262 from the large domain, and the main chain carbonyl oxygen atom and one γ carboxylate oxygen atom of Glu69 from the large domain of the adjacent subunit. As found for tryptophanase, the shell of coordinating atoms is completed by three water molecules, giving a coordination number of seven. This metal site is located about 6 Å from the active site cleft and about 18 Å from the PLP ring. The site architecture and the identities of the liganding residues are conserved in all TPLs and tryptophanases thus far sequenced. It has been reported that removal of the metal ion from E. coli tryptophanase from which PLP has been removed brings about dissociation to monomers [19,20]. Therefore it appears that the metal site makes an important contribution to subunit interactions.

While the structural data at present available for the tryptophanase and TPL metal sites are insufficient to define the structural effects that lead to inactivation of these enzymes when K^+ is either removed or replaced by Na^+, the protein residues which separate the metal site from the active site are likely to play an important role in the mechanism of activation. Inspection of Fig. 11(a) shows that the side chain of Lys256 is wedged between one of the coordinated water molecules and the phosphoryl group of PLP. Removal of K^+ and/or replacement with a smaller ion such as Li^+ or K^+ could perturb this set of interactions in such a way that the changes in orientation of the PLP ring that are believed necessary for catalysis are disturbed. Removal or replacement of K^+ could have similar effects on the position of Tyr71 (a residue from the adjacent subunit that contributes to the active site). Since each metal site and each catalytic site is formed with residues from both subunits of the dimeric unit, it may be that K^+ binding is critical for maintaining
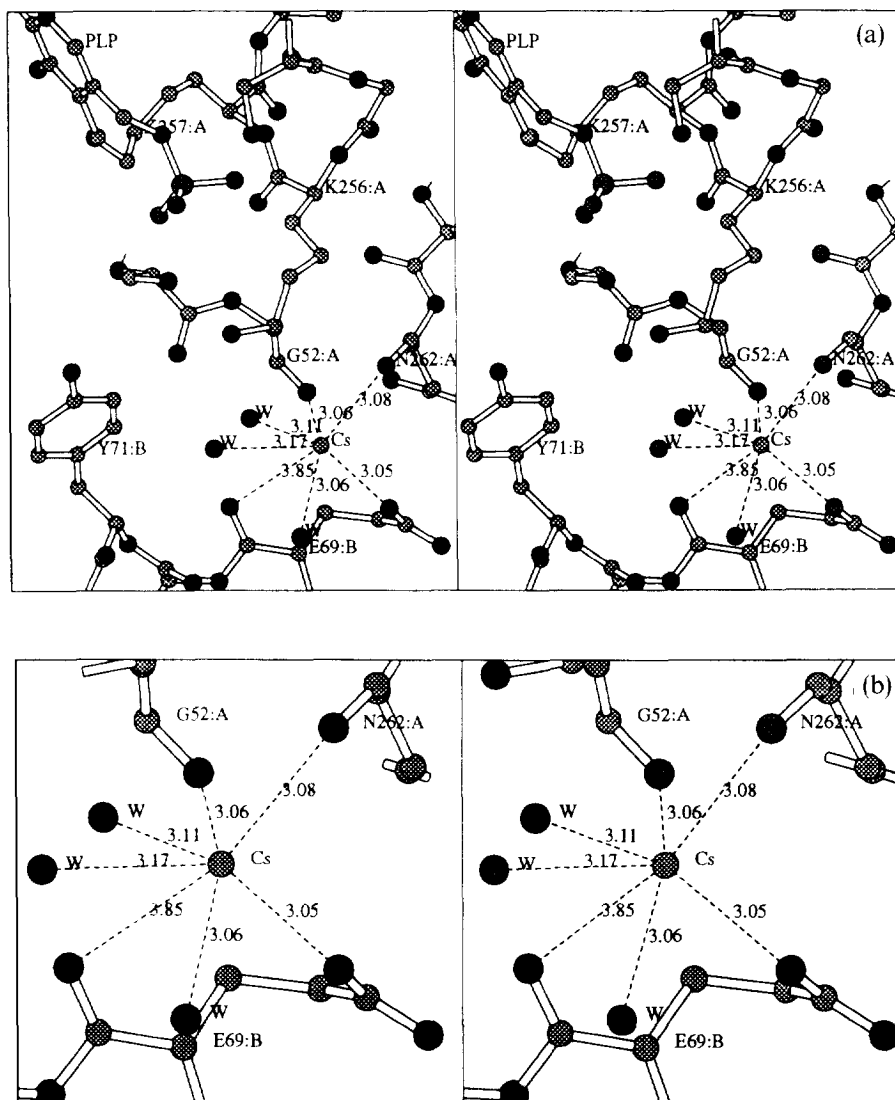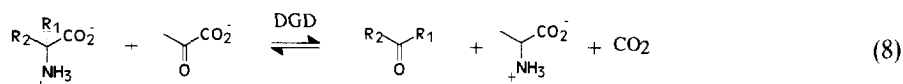
Fig. 11. Stereo drawings of the X-ray structure of Cs⁺ bound to the K⁺ site of TPL. (a) Details of the Cs⁻ complex showing the relationship of the metal ion site to the active site. PLP (upper left-hand corner) is separated from the metal site by Lys256 from subunit A and by Tyr71 from subunit B. (b) Close-up view of the bonding to Cs⁺. (Drawing provided courtesy of A.A. Antson.)

the subunit interactions that are essential for catalysis. Consequently, it seems likely that the binding of K^+ to the metal site has the effect of stabilizing the active conformation of the protein through interactions that affect PLP via Lys256 and Tyr71 and/or interactions that involve subunit contacts necessary for the integrity of the catalytic site.

4.6. Monovalent metal ion activation and inhibition of 2,2-dialkylglycine decarboxylase

4.6.1. Background

The PLP-requiring enzyme DGD is an unusual member of the α family of PLP enzymes [99] in that it uses the same active site to catalyze both transamination and decarboxylation reactions in the conversion of a 2,2-dialkylglycine and pyruvate to a new ketone, L-Ala and CO_2 [11–17]:

$$R_2 \underset{\overset{|}{NH_3^+}}{\overset{R_1}{\underset{}{C}}} CO_2^- \ + \ \underset{O}{\overset{}{\bigvee}} CO_2^- \ \underset{}{\overset{DGD}{\rightleftharpoons}} \ R_2 \underset{O}{\overset{R_1}{\bigvee}} \ + \ \underset{+NH_3}{\overset{}{\bigvee}} CO_2^- \ + \ CO_2 \tag{8}$$

The first stage of this reaction (Scheme 2) is the decarboxylation of the dialkylglycine substrate to give CO_2, ketone and PMP. The second stage is a normal transamination reaction between enzyme-bound PMP and pyruvate to give L-Ala and to regenerate enzyme-bound PLP. By taking advantage of the broad substrate specificity for amino acid derivatives with two side chain substituents at the α-carbon, Bailey and co-workers [12–14] were able to carry out a set of elegant specificity studies that provided a strong underpinning for Dunathan's hypothesis [109,110]. These studies showed that for the decarboxylation step to occur, the scissile σ bond to the carboxylate of the dialkylglycine external aldimine must be oriented perpendicular to the plane of the PLP π system so that, in the transition state, bonding overlap to include the developing p orbital in the delocalized π system is optimized. When these conditions are met, decarboxylation of the external aldimine E(Aex) (Scheme 2) to give the corresponding quinonoid E(Q1) occurs. Transfer of a proton to the C(4') atom of the quinonoid gives a ketimine E(K1) which, upon reaction with water, yields enzyme-bound PMP and the ketone product. Reaction of pyruvate with E(PMP) gives the pyruvate ketimine E(K2). The stereospecific transfer of the C(4') proton via a 1–4 prototropic shift to the C(α) atom converts the pyruvate ketimine to the external aldimine of L-Ala, and transimination with the ϵ-amino group of the active site Lys side chain (Lys272) releases L-Ala and regenerates enzyme-bound PLP.

Aaslestad and co-workers [11,15] first reported that DGD was strongly activated by K^+ and strongly inhibited by Na^- and Li^-. This initial report has only recently been followed up with solution studies to characterize this inhibition further [118]. Hohenester et al. [118] reported that the metal-free enzyme exhibits less than 0.5% of the activity found in 0.1 M KCl in the presence of 50 µM PLP (at 1 mM PLP, the metal-free enzyme is reported to exhibit about 30% activity). These workers further reported the following order of effectiveness for monovalent cation activation: $K^+ > NH_4^- > Rb^+ \gg Cs^+ > Na^+$. Li^+ was found to be totally ineffective. Jansonius' group [4,5,118] have carried out structural studies of the Li^+, Na^+, K^+ and Rb^+ complexes of DGD. The work on the Na^+ and K^+ complexes [4,5] reveal that Na^+ binding induces a large change in the conformation of the enzyme that alters the structure of the catalytic site. Li^+ binds to the same conformation stabilized by Na^+, while Rb^- binds to the K^+ conformation [118].
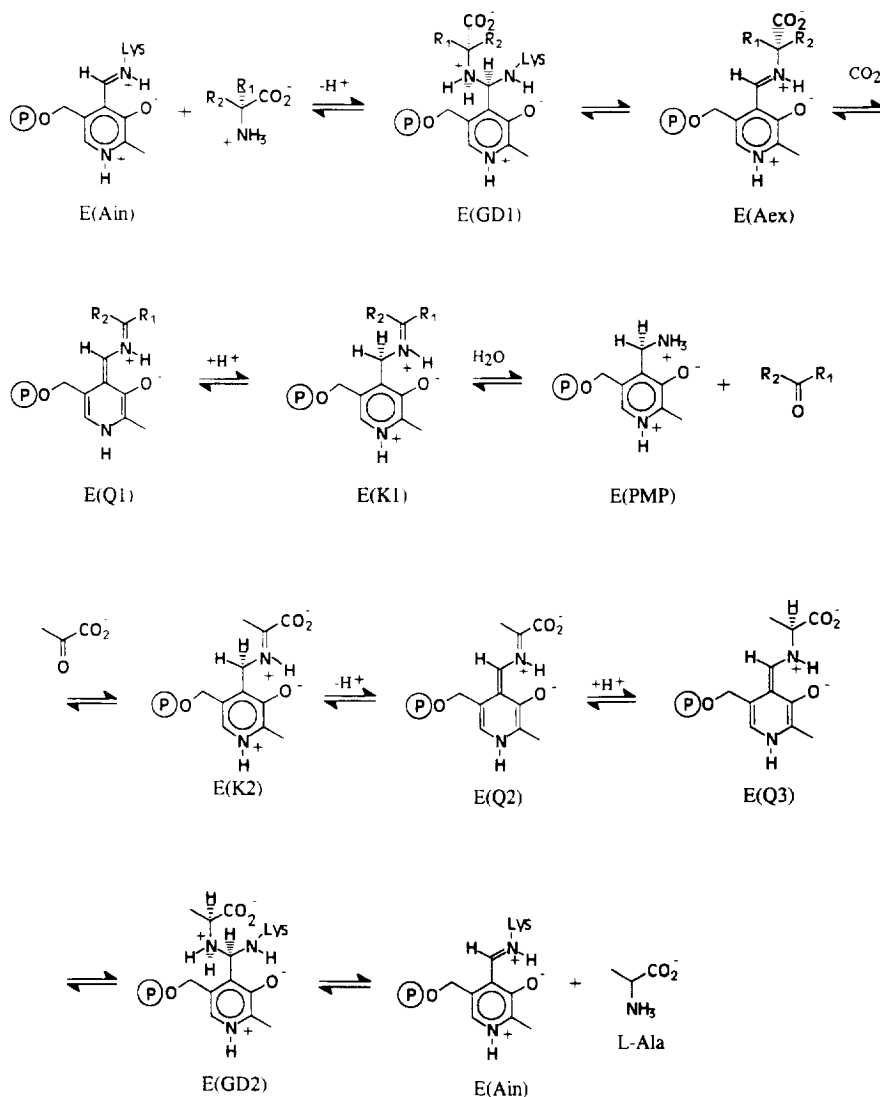
Scheme 2. Reaction pathway showing the organic structures of intermediates believed to occur in the catalytic mechanism of DGD. R_1 and R_2 are short-chain aliphatic substituents. The designations of PLP structures are the same as in Scheme 1 except that E(K1) and E(K2) are the first and second ketimine Schiff bases respectively, and PMP is pyridoxamine-5-phosphate.

4.6.2. Structural overview of 2,2-dialkylglycine decarboxylase

According to the amino acid sequence comparisons of Alexander et al. [99] and the three-dimensional structural similarity between the dimeric units of DGD, tryptophanase, TPL and various transaminases, it is clear that DGD is a member of the α family of PLP enzymes. Consequently, the overall folding of the subunits and the

monomer–monomer interactions are homologous to AspAT, tryptophanase and TPL (Fig. 12). Nevertheless, the tetrameric oligomer is assembled in a fashion that is different from that of the TPL and tryptophanase tetramers. The current work on the three-dimensional structure of DGD consists of a model that defines 93% of the protein and includes 229 water molecules, one molecule of 2-(N-morpholino)-ethane sulfonic acid buffer and two bound monovalent metal ions per subunit. The model is characterized by an R factor of 17.8% and the resolution extends to 2.1 Å. Since the molecular twofold axes coincide with the crystallographic axes, each monomer in the tetramer has the same identical conformation. The monomer (Fig. 12(a)) consists of two domains, the large domain is made up from a seven-stranded β sheet designated a–g (six parallel; strand g is antiparallel). This sheet is covered on both sides by eight α helices. The small domain consists of a four-stranded antiparallel β sheet (designated D, E, F and G) with three α helices packed against one side opposite the large domain. As found for TPL and tryptophanase, the DGD catalytic site also is located in a cleft between the large and small subunit domains near the interface between monomers of the dimeric unit, and residues from the adjacent symmetry-related monomer contribute to the active site structure. The α_4 tetrameric structure is built up as a dimer of dimers. The monomer–monomer interface has a large interaction surface. The active sites are located close to each other across the interface with the PLP rings about 15 Å apart. The dimer–dimer interface is relatively small (about one-third that of the monomer–monomer interface) and primarily involves the interaction of about ten residues from helix 6 and its N-terminal loop with symmetry-related elements. There is a hydrophobic core to this set of interactions that involves the side chains of Phe117 and Tyr119 with their symmetry-related mates. This interface also includes a few hydrogen bonds and a salt bridge (Arg196···Asp194*). As already mentioned, there is significant structural homology between the dimeric units of DGD, tryptophanase and TPL; however, the dimer–dimer interface of DGD is completely different from those of tryptophanase and TPL. The DGD interface is formed from the "bottom" of the dimer while, in tryptophanase and TPL, it is the "top" surface that forms the interface.

At the active site, PLP is covalently bound in a cleft of the enzyme via a Schiff base linkage to Lys272. The PLP N-1 is hydrogen bonded to the Asp243 side-chain carboxylate, the PLP 3-oxygen atom is hydrogen bonded to the carboxamide side-chain NH of Gln243 and to the protonated Schiff base nitrogen atom of the internal aldimine, and the PLP phosphoryl group has nine hydrogen bonds to the amide NH protons of Gly111, Ala 112 and Thr303* (asterisks indicate residues from the adjacent subunit), the OH of Thr303* and five ordered water molecules. The positive end of the macrodipole of helix 4 is directed toward the phosphoryl group, but there is no group with a formal positive charge in close proximity to this group. The PLP pyridine ring makes van der Waals contact with the side chains of Ala245 (back side) and Trp138. The plane of the indole ring of Trp138 is placed at 25° to the plane of the PLP ring, and the ring NH is hydrogen bonded to one of the water molecules that is hydrogen bonded to the phosphoryl group. One face of the indole ring forms a surface that is probably part of the substrate binding site.

Model building to investigate possible modes of substrate binding to the site
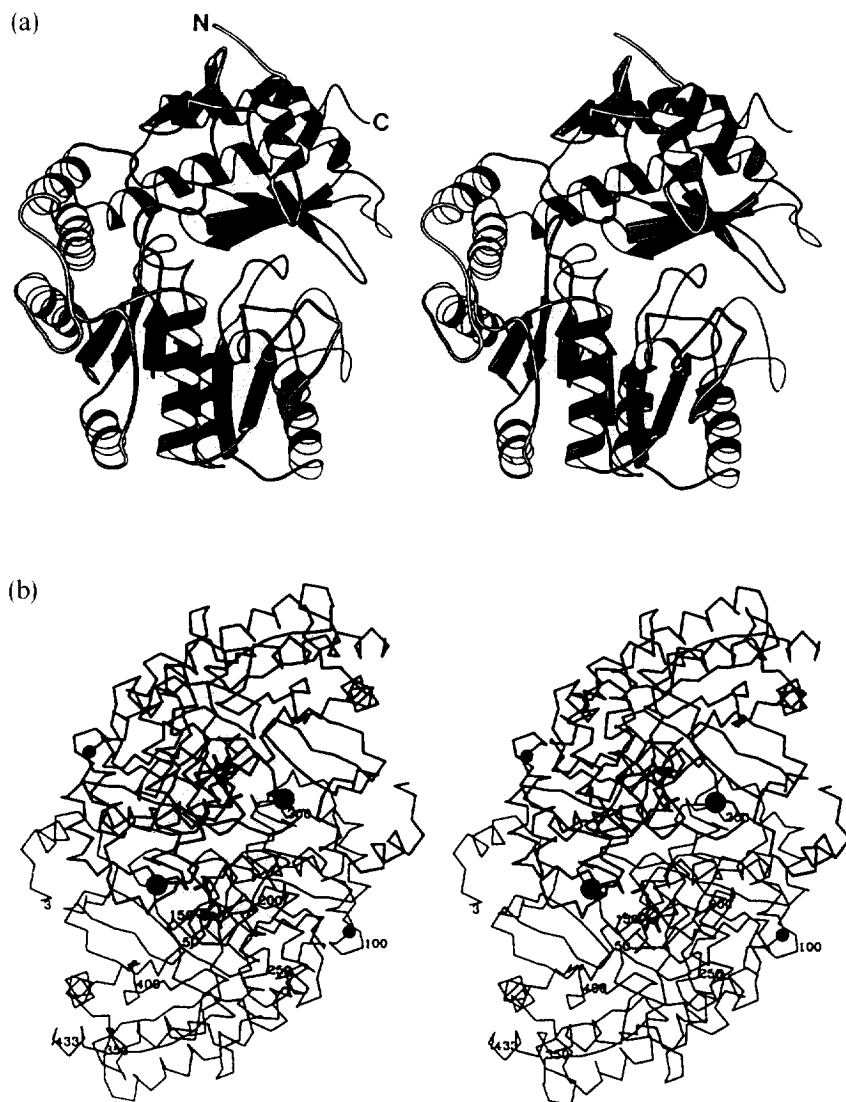
(a)

(b)

Fig. 12. Stereo drawings of (a) the DGD monomer and (b) the DGD dimer. (a) Ribbon drawing of the DGD monomer showing the folding motifs of the large PLP binding domain (bottom) and the small domain (top), the domain contacts and the N and C termini. (b) α-Carbon drawing of the DGD dimer viewed along the dimer twofold axis. One monomer is drawn with thin lines, and the other with thick lines. Every fiftieth residue in one subunit is labeled. The PLP cofactors are drawn in bold. Large and small full circles represent the ions bound at sites 1 and 2 respectively. (Taken from Ref. [5] with permission.)

during the decarboxylation half-reaction indicate that the substrate carboxylate (e.g. L-isovaline) could form hydrogen bonds to the guanidinium and ammonium ion side-chain groups of Arg406 and Lys272. In accord with Dunathan's hypothesis [109,110], these interactions would stabilize the binding of substrate in a conformation which places the carboxylate in the correct orientation with respect to the PLP π system for decarboxylation. This orientation also places the substrate carboxyl group close to the side chain carboxamide of Gln52, perhaps within hydrogen bonding distance.

In the transamination half-reaction, the scissile α-CH bond of the substrate must be oriented perpendicular to the PLP ring so that the α-proton can be removed by the action of the active site base. When L-Ala is modeled into the site so that this orientation is obtained, the ε-amino group of Lys272 is correctly positioned to act as the general base catalyst to abstract this proton. Crystallographic and solution mechanistic studies of AspAT [63–66,105] have demonstrated that the analogous Lys residue (Lys258) in AspAT is similarly situated and plays this mechanistic role.

4.6.3. Crystallographic studies of the 2,2-dialkylglycine decarboxylase monovalent metal ion binding sites

The elegant crystallographic work of Toney et al. [4,5] has identified the K^+ site as responsible for the activation of DGD (Fig. 13). These workers have shown that there are two monovalent metal ion sites in each DGD subunit; one is located close to the catalytic site which shows selectivity for K^+ (site 1), and the other site is more remote from the active site and prefers Na^+ over K^+ (site 2). Two crystal structures have been described [4,5]: a structure where K^+ is bound to site 1 and Na^+ is bound to site 2, and a structure where Na^+ is bound to both sites. Comparison of these two structures (Fig. 13) shows that the protein structure in the vicinity of site 1 undergoes a change in conformation when K^+ is substituted by Na^+. This conformational change propagates to the active site and causes rearrangements in the positions of two residues: Ser80, which was a ligand to K^+, is displaced by a water molecule, and the position of Tyr301, a residue in the active site, is shifted. Smaller changes in the positions of other site residues are also seen. The conformation change causes a $1°$ rotation of the subunits with respect to each other which slightly affects the domain contacts between subunits. Since site 2 is unaffected by this substitution, and since K^+ activates while Na^+ inhibits DGD, it is logical to conclude that the conformational change associated with the replacement of K^+ by Na^+ at site 1 is directly linked to the opposing effects of these metal ions on the activity of the enzyme.

Stereo drawings of site 1 complexes with K^+ and Na^+ are shown in Fig. 13. In the K^+ complex (Fig. 13(a)), the K^+ coordination sphere is made up of six donor atoms, the backbone carbonyl oxygen atoms of Leu78, Thr303 and Val305, the side-chain hydroxyl oxygen atom of Ser80, one oxygen atom from the side chain carboxylate of Asp307 and one water molecule. The $K^+\!-\!O$ bonds to the carbonyl oxygen atoms range from 2.70 to 2.87 Å, the bond to the Ser oxygen atom is 2.84 Å, the bond to water is 2.73 Å and the bond to the carboxylate oxygen atom is 2.47 Å. The shorter bond to the carboxylate oxygen atom is expected on electrostatic grounds, and the orientation of this carboxylate–K^+ bond is classified as "side-on
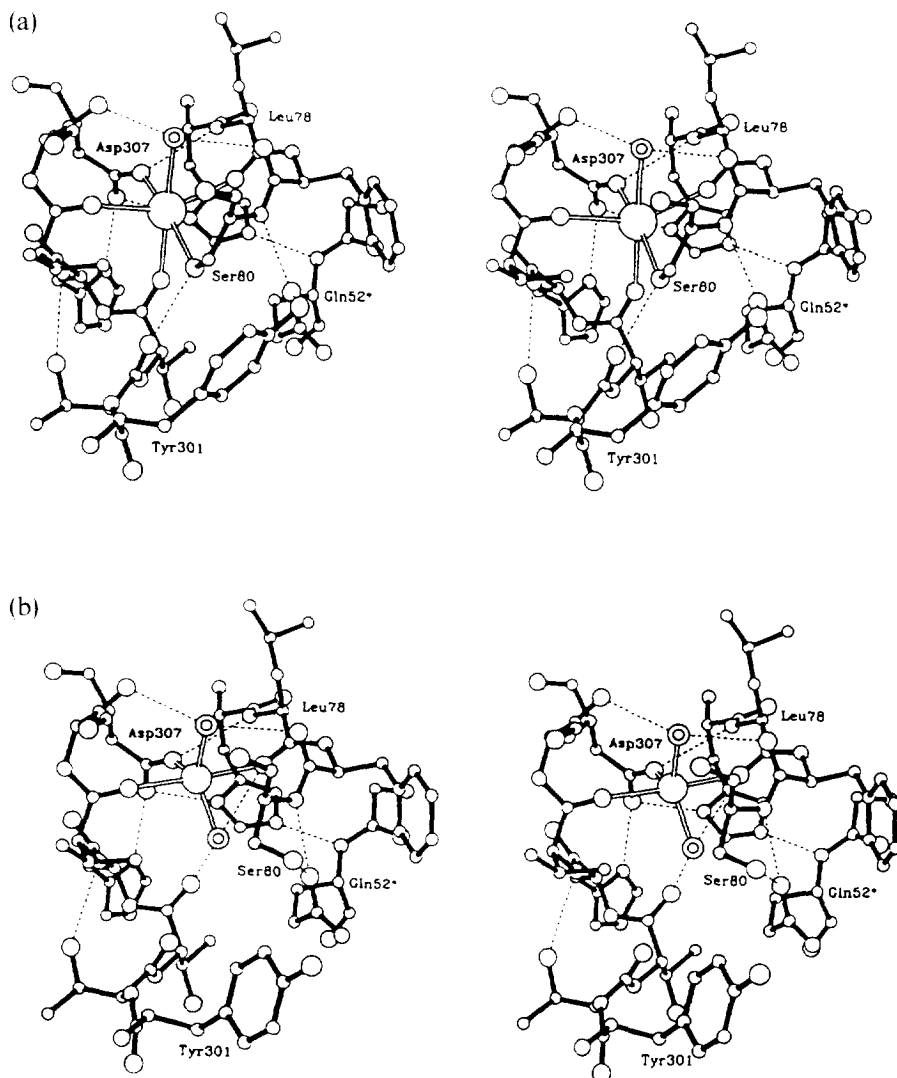
(a)

(b)

Fig. 13. Stereo drawings showing the details of coordination for metal binding site 1 in DGD: (a) K⁺ complex; (b) Na⁺ complex. The metal ions are represented by large open circles, and the water molecules by double circles. The broken lines indicate hydrogen bonds. All ligands to both metal ions are oxygen atoms. K⁺ is six coordinated with octahedral geometry and an average metal–ligand distance of 2.72 ± 0.14 Å. Na⁺ is five coordinated with trigonal bipyramidal geometry and an average metal–ligand distance of 2.33 ± 0.16 Å. Residues contributed by the second subunit in the dimer are labeled with an asterisk. Note that the change in coordination structure causes changes in the conformation of Ser60 and Tyr301 and shifts of other residues (see text). (Taken from Ref. [5] with permission.)

syn" [119]. The water molecule makes hydrogen-bonding interactions with the carbonyl oxygen atom of Phe79 and the carbonyl oxygen atom of Ser306. In this structure, the Ser80 main-chain carboxamide nitrogen is hydrogen bonded to the side-chain carbonyl oxygen atom of Gln52.

In the Na^+ complex (Fig. 13(b)), the cavity adjusts to a five-coordinated structure to accommodate the smaller size of Na^+, and this change is accompanied by a slight displacement of the metal ion, a large rearrangement of the coordination sphere and a large change in the conformation of the protein. The donor atoms consist of the main-chain carbonyl oxygen atoms of Leu78 and Val305, one carboxylate oxygen atom of Asp307 and two water molecules. The Leu78 Na^+ —O bond length is 2.36 Å, while the Val305 bond length is significantly longer, 2.60 Å. The bonds to the two water molecules are 2.23 and 2.19 Å, while the bond to Asp307 is 2.27 Å. The distances to the carbonyl oxygen atom of Thr303 (4.04 Å) and the hydroxyl oxygen atom of Ser80 (5.92 Å) are too far away to be considered bonds to Na^+. This change in coordination from the K^+ complex is achieved by rotation of the side-chain oxygen of Ser80 by about 120° and by moving the carbonyl oxygen of Thr303 away from Na^+ to accommodate the second water molecule. Model building studies indicate that (without significant rearrangement of the protein backbone) the donor atoms which define the K^+ cavity could not contract to accommodate the smaller radius of the Na^+ ion; a shortening of the bonds by 0.3–0.4 Å would violate the van der Waals distances between the side chain of Ser80 and the carbonyl of Thr302. The second water molecule is buried in the protein structure and makes hydrogen-bonding interactions with the carbonyl oxygen atom of Thr303 and Leu78. The slight repositioning of the metal ion causes residues 300–305 to move as a segment. These alterations of the metal ion cavity and rearrangement of the coordination sphere cause a slight expansion of the protein structure in the vicinity of the metal site and reorientation of the side chains of Tyr301 and Ser80. The rotation of the Ser80 side chain allows both the main-chain carboxamide nitrogen atom and the side-chain hydroxyl to form hydrogen bonds with the side-chain carboxamide of Gln52. Hohenester et al. [118] have extended these structural studies to determination of the crystal structures of the Li^+ and Rb^+ complexes. While the X-ray scattering factor for Li^+ (2) is too small to allow direct detection of Li^+, calculation of difference electron density maps comparing the Li^+, Na^+, K^+ and Rb^+ complexes gave strong indirect evidence for Li^+ bound to site 1. These studies establish that Li^+ stabilizes the conformation favored by Na^+, while Rb^- stabilizes the conformation favored by K^+. They conclude that the high activity form of DGD is stabilized by monovalent cations with effective ionic radii of 1.3–1.5 Å, while smaller ions stabilize the low activity form. Therefore the switch between these forms is a cation-size-dependent phenomenon.

4.6.4. Implications of the conformational change to catalysis

For the decarboxylation half-reaction, the productive complex of bound substrate probably forms three hydrogen bonds: one to the carboxamide side chain of Gln52, one to Arg406 and one to Lys272. It appears that the conformational change resulting from Na^+ or Li^+ substitution for K^+ at site 1 would alter these interactions between

site and substrate. Toney et al. [4,5] and Hohenester et al. [118] propose that the inhibitory effects of Na⁻ substitution result from the change in the conformations of Ser80 and Tyr301 which may disrupt the productive binding of substrate. It seems likely that this change in conformation drives the enzyme to an inactive form (or low activity form) in which the bound substrate and the site functional groups and/or the PLP ring are improperly aligned for catalysis. However, at this stage of the structural and mechanistic investigations, it is not known which steps in the catalytic mechanism are inhibited by Na^+. AspAT undergoes interconversion between open and closed conformations during the catalytic cycle. If a similar conformational transition is obligatory for catalysis in DGD, then it could be that Na^+ inhibits this process. However, no evidence has been reported for such a conformational transition in DGD. Alternatively, it might be that the protein conformation stabilized by Na^+ is unable to undergo one or more conformational transitions associated with the interconversion of covalent intermediates along the catalytic path.

The work of Toney et al. [4,5] and Hohenester et al. [118] provides an important breakthrough in our efforts to understand the relationship between structure and function in MMA enzymes. Nevertheless, further structural and solution studies are needed to achieve a detailed explanation for the K^+-mediated activation and Na^+-mediated inhibition of DGD.
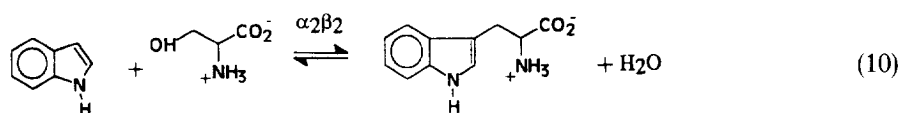
4.7. Monovalent metal ion activation of tryptophan synthase
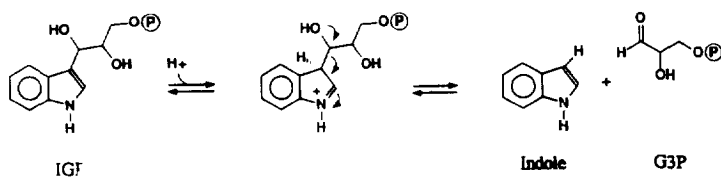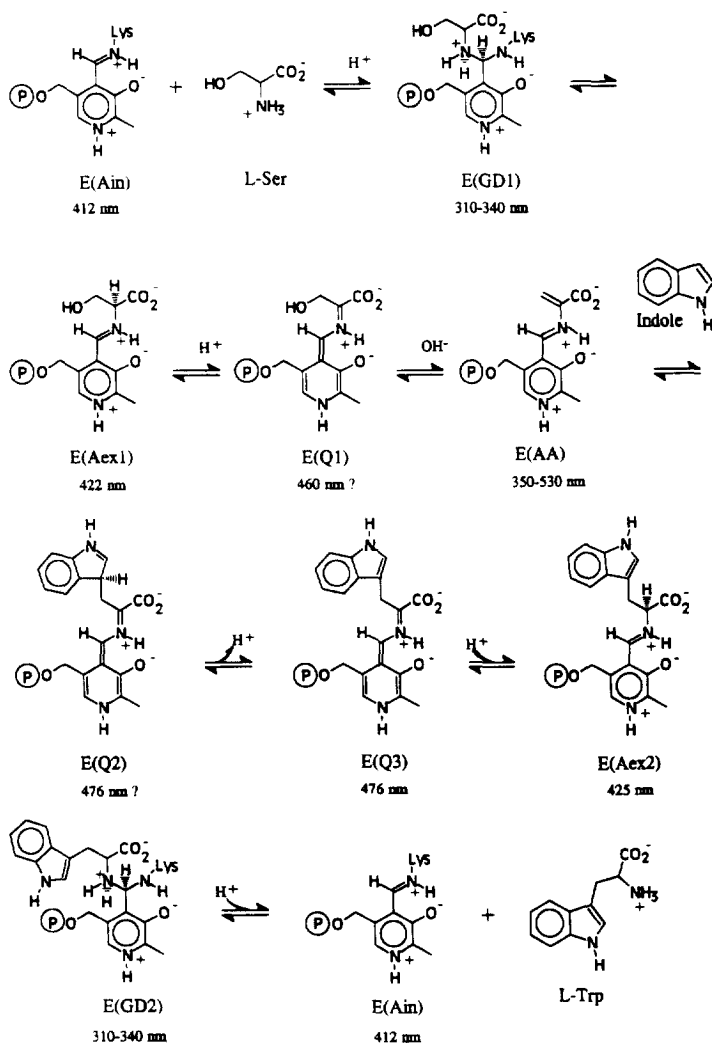
4.7.1. Background

The tryptophan synthases from enteric bacteria are bienzyme complexes with a tetrameric $\alpha_2\beta_2$ subunit composition. Subunits are arranged in a linear $\alpha\beta\beta\alpha$ oligomeric structure with a total length of about 150 Å [120,121]. The active sites of neighboring α and β subunits are separated by about 25–30 Å and are interconnected by a tunnel that serves as the conduit for the transfer of the common metabolite, indole, between the two active sites of the bienzyme complex [71,120]. The complex catalyzes the last two steps in the biosynthesis of tryptophan (Scheme 3) [101,102,106]. The α subunit cleaves 3-indole-D-glycerol 3'-phosphate (IGP) to α-glycerolphosphate (G3P) and indole; this is the α reaction:


$$\text{(9)}$$
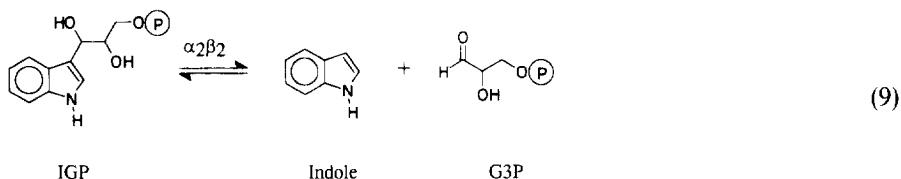
The β subunit requires PLP and catalyzes the replacement of the β-hydroxyl of L-Ser by indole to form L-Trp and a water molecule; this is the β reaction:

$$\text{(10)}$$

α-Reaction

IGP   Indole   G3P

β-Reaction

E(Ain)   L-Ser   E(GD1)
412 nm   310-340 nm

E(Aex1)   E(Q1)   E(AA)
422 nm   460 nm ?   350-530 nm

E(Q2)   E(Q3)   E(Aex2)
476 nm ?   476 nm   425 nm

E(GD2)   E(Ain)   L-Trp
310-340 nm   412 nm

The overall reaction, synthesis of L-Trp from IGP and L-Ser is designated as the $\alpha\beta$ reaction:

$$+ H_2O \tag{11}$$
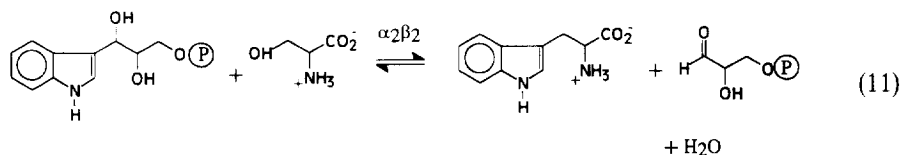
The coordination of catalytic events at the α and β sites is ensured by a set of allosteric interactions across the α–β subunit interface [71–74,111,122–129]. Both ligand binding and covalent reactions play allosteric roles in site–site communication. One example of such allosteric communication is the activation of the α catalytic site by formation of the α-aminoacrylate intermediate at the β site [73,123,126,127].

The recent studies of Peracchi et al. [28,29] and work from this laboratory [30,31] have demonstrated that the native $\alpha_2\beta_2$ enzyme is activated by the binding of monovalent cations to a specific site on the protein. Early work [1,101,102,130–134] and the recent study of Yang and Miles [135] had shown that the catalytic properties of the β_2 dimer are altered by the binding of some monovalent cations (especially K^+ and NH_4^+, but not Na^+ [1,101,102,130]). It is not clear why the $\alpha_2\beta_2$ species was only recently shown to be an MMA enzyme [28,30,31]. As will be shown below, at 25 °C Na^+, K^+ and NH_4^+ all activate both the $\alpha\beta$ and β reactions; these ions help to ensure the catalytic efficiency of the bienzyme complex and they play an essential role in mediating allosteric interactions between subunits.

4.7.2. Structural features of $\alpha_2\beta_2$ tryptophan synthase

The three-dimensional structure of the $\alpha_2\beta_2$ complex from *Salmonella typhimurium* has been solved to 2.5 Å resolution [120,121]. The catalytic competence of the crystalline enzyme has been demonstrated [136,137]. The smaller α subunit is an eightfold α–β barrel (Fig. 14) [120]. The larger β subunit contains the PLP cofactor [120]. The β subunit consists of two domains (Fig. 14), which are very similar in size and folding motif. The N-terminal domain is largely derived from residues 1–204, the C terminal is largely comprised of residues 205–397. Residues 53–85 extend between the two domains. The core structure of the N domain consists of four strands arranged in a parallel fashion with a left-hand twist. Three helices are packed on one side of the sheet; a fourth extends across the back of the sheet. The C-domain core is built in a similar fashion. A five-stranded, strongly twisted sheet is packed between helices. The dipole of one of the helices on the interior side is oriented to

Scheme 3. Organic structures of the intermediates in the reactions catalyzed by the tryptophan synthase $\alpha_2\beta_2$ bienzyme complex. The α reaction is the reaction catalyzed by the α subunit. The β reaction is the reaction catalyzed by the β subunit. Where known, the absorption maxima of the long-wavelength absorption bands of each intermediate are given. The designations used for PLP structures are the same as in Scheme 1. Note that the β reaction occurs in two stages: stage I consists of the reaction of L-Ser to give E(AA) and a water molecule; stage II is the reaction of E(AA) with indole to yield L-Trp and to regenerate E(Ain).
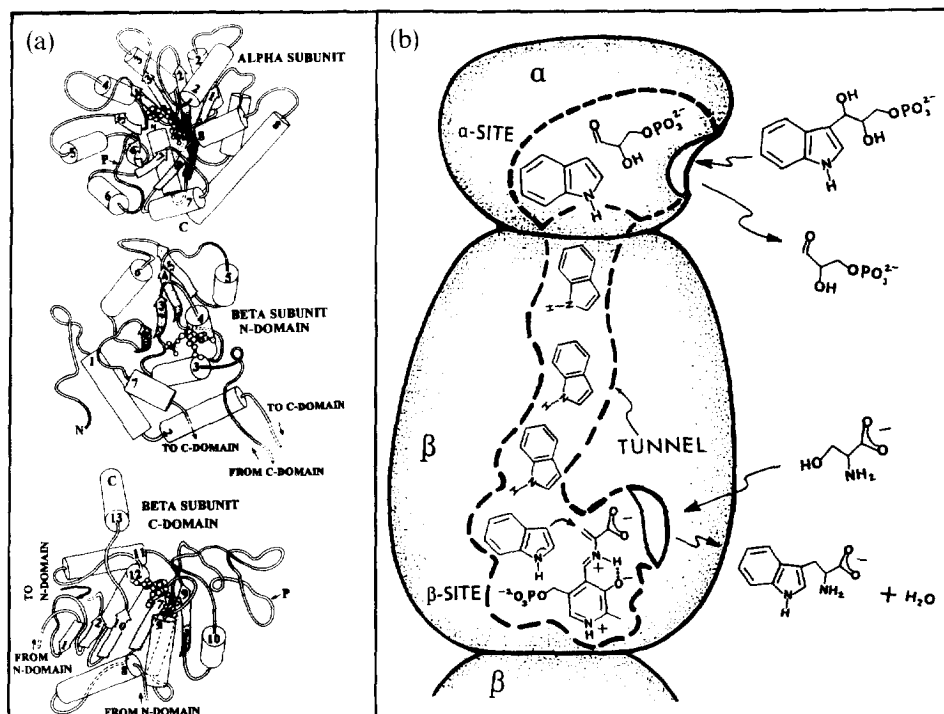
Fig. 14. (a) Cartoon representations of the arrangement of helices, sheets and loops in the α-subunit, and the N-terminal and C-terminal domains of the β subunit of *S. typhimurium* tryptophan synthase. The catalytic site of the α subunit is filled with the IGP analogue indole-3-propanol phosphate (○). The PLP binding site is located at the domain–domain interface and is indicated by open circle structures. (Taken from [120] with permission.) (b) Cartoon depicting the active sites of the α and β subunits, the interconnecting tunnel, the sequence of reactions, and the routes of entry and exit of substrates and products for the αβ reaction (see Scheme 3). (Taken from Ref. [71] with permission.)

stabilize the bound phosphoryl group of PLP. A region with less well-defined secondary structure forms extended hairpin loops. This region forms the contacts with the α subunit and part of the interconnecting tunnel. The PLP binding site is located at the interface between the N and C domains at the center of the subunit. The phosphoryl group forms several hydrogen bonds to the backbone. The Schiff base internal aldimine form of the coenzyme is in cis configuration so that the imine nitrogen and the 3'-hydroxyl oxygen atom of the coenzyme are in close proximity. While the loci of the monovalent metal ion binding site(s) have not yet been described, it is unlikely that there will be any homology to the sites reported for tryptophanase, TPL or DGD. The folding topologies of the α and β subunits are completely different from these enzymes, and therefore the metal ion binding site also must be different. Because the β_2 form of the enzyme also is subject to monovalent metal ion activation [1,101,102,130–134], we presume that the metal ion site responsible for activation of $\alpha_2\beta_2$ is located on the β subunit.

4.7.3. Solution mechanistic studies of monovalent metal ion effects on $\alpha_2\beta_2$ tryptophan synthase

The UV–visible absorbance properties of the PLP coenzyme provide excellent signals for dissection of catalytic mechanism and elucidation of allosteric effects in the tryptophan synthase system [101,102,71–76,122]. These spectroscopic signatures have been exploited to investigate the function and mechanism of monovalent metal ion effects in this system by Peracchi et al. [28,29] and ourselves [30,31]. Peracchi et al. [28,29] were the first to recognize that $\alpha_2\beta_2$ is an MMA system and they have extensively studied the effects of monovalent metal ions by phosphorescence decay spectroscopy for the $\alpha_2\beta_2$ species, and by equilibrium and steady state kinetic methods for the reaction of L-Ser with the $\alpha_2\beta_2$ bienzyme complex, both in solution and in $\alpha_2\beta_2$ crystals (Fig. 15). The average decay lifetime of the phosphorescence of Trp177 in the β subunit is increased in the presence of Li^+, Na^+, Cs^+ or NH_4^+, indicating a decrease in the flexibility of the N domain of the β subunit. They also found that the intensity of the 412 nm spectral band of E(Ain) (attributed to a polar environment) increases in the presence of either Na^+ or Cs^+, while the band at 350 nm (attributed to a less polar environment) concomitantly decreases. Furthermore, as shown in Fig. 15, the binding of monovalent metal ions, both in solution and in the crystalline enzyme, alters the equilibrium distribution of the enzyme-bound external aldimine E(Aex1) and the α-aminoacrylate E(AA) species. At both 10 and 20 °C, the binding of Na^+ or K^+ shifts the equilibrium in favor of E(Aex1) (Fig. 15), and these effects are dependent on pH. Li^+, Rb^+ or Cs^+ binding causes the appearance of a 470 nm absorbance band attributed to E(AA) (Fig. 15). The apparent k_{cat} values and K_m values for indole in the β reaction are also affected. The effect on K_m is dramatic; at 10 °C, values range from 145 μM in the absence of

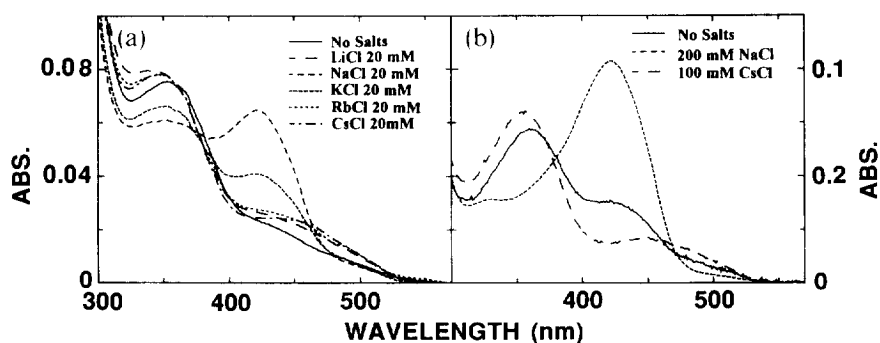

Fig. 15. Absorption spectra of L-serine-$\alpha_2\beta_2$ complexes in the presence and in the absence of monovalent cations (a) in solution and (b) in the crystalline state. Absorption spectra were recorded for a solution containing the $\alpha_2\beta_2$ complex (0.5 mg ml^{-1}), 50 mM L-Ser, 25 mM Bis–Tris propane, 1 mM EDTA, at pH 8 and 10 °C, in the absence and in the presence of Li^+, Na^+, K^+, Rb^+ or Cs^+. Single-crystal polarized absorption spectra were recorded with the electric vector of the linearly polarized light parallel to the x optical axis [137]. The crystal was suspended in a solution containing 25 mM Bis-Trsi propane, 20% PEG 8000 M$_r$, 1 mM EDTA, 50 mM L-Ser, at pH 7.6 and 20 °C, both in the absence and in the presence of Na^+ and Cs^+. (Taken from Ref. [28] with permission.)

metal ion to 7.5 µM in the presence of Na^+, while k_{cat} ranges from 0.68 s^{-1} in the absence of metal ion, to 3.62 s^{-1} in the presence of Cs^+. They conclude that the binding interaction which perturbs the spectrum of E(AA) is responsible for activation of the β reaction. The order of effectiveness in activating the β reaction at 10 °C, as measured by the increasing values of k_{cat}/K_m, was found to be $Cs^+ > Li^+ > K^+ > Na^+$, whereas at 20 °C this order of effectiveness is reversed. These results indicate a dependence of the rate-limiting step on temperature, and therefore a distinct action of individual cations on different catalytic steps [28,29].

In a series of independent studies at pH 7.8, Woehl and co-workers [30,31] found that monovalent metal ions are essential both for the reaction of nucleophiles with E(AA) (Fig. 16) and for the allosteric activation of the α site by formation of E(AA) at the β site. In an effort to understand the roles played by monovalent metal ions in the structure and function of $\alpha_2\beta_2$, we have undertaken a detailed set of rapid-scanning stopped-flow (RSSF) absorbance and single-wavelength stopped-flow (SWSF) absorbance and fluorescence kinetic and equilibrium binding studies to examine the effects of Na^+ and K^+ on the β and αβ reactions at 25 °C. The effects on the α reaction have been examined using steady state kinetic methods. Both RSSF and SWSF spectroscopies have proven to be very useful in defining the effects of Na^+ and K^+ on the transient pre-steady state and steady state events that occur during the catalytic cycles of these reactions.

The time-resolved set of RSSF spectra collected during the pre-steady state and steady state phases of the αβ reaction are shown in Fig. 17. In this experiment, $\alpha_2\beta_2$ is reacted with a mixture of L-Ser and IGP in the absence (Fig. 17) and presence (Fig. 17) of Na^+. In the absence of Na^+, only a small amount of E(AA) turns over. The steady state spectrum (spectrum 25) is dominated by the spectrum of E(AA). In the presence of Na^+, however, almost all the E(AA) species is reactive, and a large fraction of the enzyme is converted to the E(Aex1) species ($\lambda_{max} = 425$ nm) in the pre-steady state phase of the reaction (spectra 1–8). Fluorescence kinetic studies confirm that the species which accumulates in the transient phase is E(Aex1) and not E(Aex2) (Scheme 3). The RSSF data (Fig. 17) establish that the steady state is
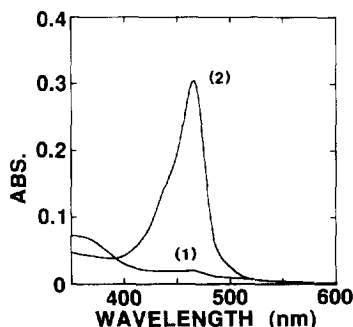

Fig. 16. UV–Visible quasi-static absorbance spectra of the quinonoid formed in the reaction of 6 µM $\alpha_2\beta_2$ with 40 mM L-Ser and 2 mM indoline (an indole analogue [138]) in the absence (curve (1)) and in the presence (curve (2)) of 100 mM Na^+.
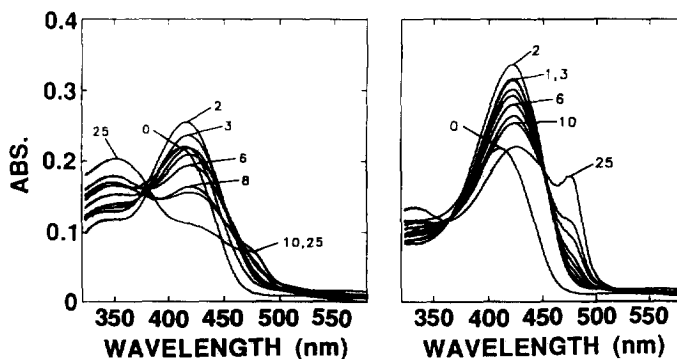
Fig. 17. RSSF spectra for the reaction of $\alpha_2\beta_2$ with L-Ser and IGP (the $\alpha\beta$ reaction; see Eq. (11) and Scheme 3) in the absence (left) and in the presence (right) of 100 mM Na$^+$ (concentrations: $[\alpha_2\beta_2]=$ 18 µM; [L-Ser] = 40 mM; [IGP] = 0.5 mM). The numbered spectra are taken at the following time points after flow stopped: spectrum 0, 0 s; spectrum 2, 0.017 s; spectrum 3, 0.026 s; spectrum 4, 0.034 s; spectrum 5, 0.043 s; spectrum 6, 0.06 s; spectrum 8, 0.094 s; spectrum 10, 0.128 s; spectrum 25, 1.709 s.

dominated by E(Aex1) with some E(Q) species also present ($\lambda_{max} = 476$ nm). Similar results were obtained for the β reaction, and in the reaction of IGP with L-Ser. When the reaction of $\alpha_2\beta_2$ with L-Ser only was examined by RSSF and SWSF absorbance and SWSF fluorescence spectroscopies, we found that reaction occurs with a large transient yield of E(Aex1) in the presence of Na$^+$ or K$^+$, but almost none is detected in the absence of monovalent metal ions.

The results of these rapid kinetic studies can be summarized as follows.

(1) The amount of E(Aex1) species that transiently accumulates is greatly enhanced when monovalent metal ions (Na$^+$ or K$^+$ at 25 °C and pH 7.8) are bound to $\alpha_2\beta_2$. In the absence of metal ions, the E(Ain) species turns over to the E(AA) species without significant accumulation of E(Aex1).

(2) In the absence of metal ions, the E(AA) species is very unreactive toward nucleophiles; E(AA) is the predominant form of the enzyme in the steady state phases of all the reactions. When Na$^+$ or K$^+$ is bound, E(AA) reacts readily with indole and other nucleophilic analogues of indole, and spectra measured in the steady state phase are dominated by E(Aex1) and some E(Q).

SWSF absorbance and fluorescence measurements for these same reactions establish that the relaxation rates of individual steps observed in the transient or pre-steady state phases of the reactions are altered by metal ion binding. In the presence of Na$^+$, the formation of E(Aex1) in the reaction of L-Ser with $\alpha_2\beta_2$ is speeded up 3.7-fold, while the decay of E(Aex1) to E(AA) is slowed down about threefold. Steady state activity measurements for the α, β and $\alpha\beta$ reactions gave the following results.

(1) In the absence of monovalent metal ions, the α and $\alpha\beta$ reactions show essentially identical turn-over rates, indicating that the α reaction is rate determining for turn-over under these conditions.

(2) In the presence of metal ions, the turn-over rate of the α reaction (in the absence of L-Ser) is decreased to 30% of that measured in the absence of metal ions.

(3) Nevertheless, the turn-over rate of the $\alpha\beta$ reaction is stimulated eightfold or tenfold in the presence of K^+ or Na^+ respectively.

(4) The β reaction is also stimulated fivefold or tenfold by K^+ or Na^+ respectively. This corresponds to fifteenfold or thirtyfold stimulation of the α reaction by the combined effects of L-Ser and K^+ or Na^+ respectively. Brzovic et al. [73] have shown that the conversion of E(Aex1) to E(AA) in the presence of monovalent metal ions is the chemical trigger for activation of the α site. These studies [30,31] establish that metal ion binding is essential for this activation. Without a monovalent cation bound to the enzyme, E(AA) is unable to trigger the conformational transition that activates the α site.

The available structural and solution studies of $\alpha_2\beta_2$ and its complexes provide a strong case for two types of conformational transition in the protein.
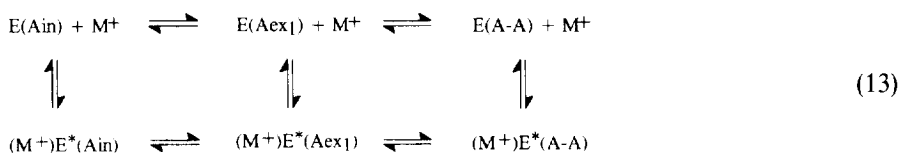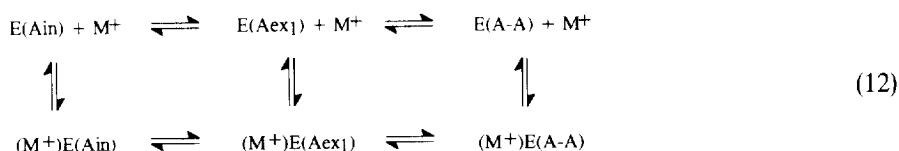
(a) Localized conformational changes in the β site that are obligatory to catalysis appear to correspond to structural transitions that are necessary for lowering the activation energies of the various covalent transformations (at least nine; see Scheme 3) which occur in the catalytic cycle, via Pauling strain distortion interactions [60,61,71–76,138–141].

(b) More global conformational changes that are mediated by allosteric interactions appear to involve interconversion between open and closed conformations of the protein in which one or the other or both of the α and β subunits undergo transitions between open (low activity) and closed (high activity) forms. The purpose of these conformational transitions has been postulated to be twofold: ligand-mediated interconversion between open (inactive) and closed (active) forms provides a mechanism for coupling the reactions at the α and β active sites so that catalysis occurs in phase [30,31,71–74,111,122,141], and interconversion between open and closed forms prevents the escape of indole from the interconnecting tunnel, thereby ensuring that the fate of indole is conversion to L-Trp [71–74,111]. Finally, there are points of linkage between the localized conformational transitions at the α and β sites and the more global changes between open and closed subunit conformations [71–74,111]. The binding of monovalent metal ions is essential for this linkage.

In the models discussed below, it is shown that a switch between two conformations of the enzyme is the likely mechanism of action for monovalent metal ion effects on $\alpha_2\beta_2$. These conformational changes are probably of a more localized nature than the opening and closing of subunits. Preliminary work [142] indicates that metal ion binding does not switch the enzyme between open and closed conformational states. These metal-ion-driven conformational transitions are probably similar to the more subtle changes that have been documented for DGD (see Fig. 13) [4,5,118]. The discussion of the theoretical basis for monovalent metal ion effects in the first section of this review postulates dynamic and structural roles. Both of these elements possibly are important to components of the metal ion effects on $\alpha_2\beta_2$.
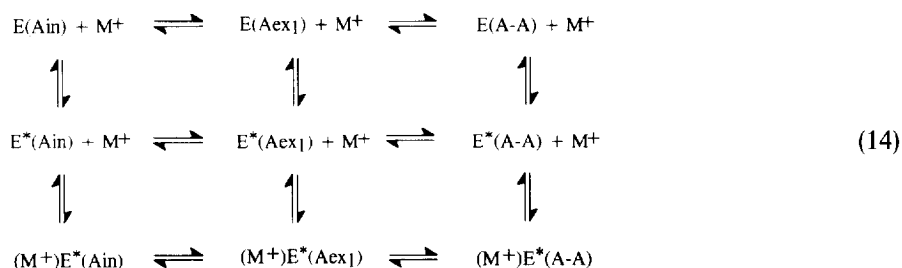
Through simulation studies of the kinetic time courses to test possible mechanisms, we have found that the rate changes which occur in the first stage of the β reaction (the reaction of L-Ser) require the existence of two forms of the enzyme with different sets of rate constants for the chemical transformations. The differences in activation energies for the two forms becomes especially striking in the case of the reaction of

the E(AA) with indole. One form of the enzyme proves to be essentially inactive in that step. Because both enhancement and reduction of relaxation rates are found in the reaction of L-Ser with the enzyme, the observed rate changes cannot be explained by a metal ion concentration dependency. In the dynamic picture the bound metal ion changes the relative position of transition-state vs. ground-state energies:

$$
\begin{array}{ccccc}
E(Ain) + M^+ & \rightleftharpoons & E(Aex_1) + M^+ & \rightleftharpoons & E(A\text{-}A) + M^+ \\
\updownarrow & & \updownarrow & & \updownarrow \\
(M^+)E(Ain) & \rightleftharpoons & (M^+)E(Aex_1) & \rightleftharpoons & (M^+)E(A\text{-}A)
\end{array}
\tag{12}
$$

$$
\begin{array}{ccccc}
E(Ain) + M^+ & \rightleftharpoons & E(Aex_1) + M^+ & \rightleftharpoons & E(A\text{-}A) + M^+ \\
\updownarrow & & \updownarrow & & \updownarrow \\
(M^+)E^*(Ain) & \rightleftharpoons & (M^+)E^*(Aex_1) & \rightleftharpoons & (M^+)E^*(A\text{-}A)
\end{array}
\tag{13}
$$

This results in a different set of rate constants for the metal-bound and metal-free enzyme species. Considering the effects of metal ion binding on both the α and the $\alpha\beta$ reactions and on the phosphorescence properties of the protein [28–31], it is apparent that metal ion binding is accompanied by a change in the conformation of the enzyme. Two possible pathways based on the above inferences are shown in the two reactions in Eqs. (12) and (13).

The preferential binding of the metal ion to one of two pre-existing conformations of the enzyme provides an alternative way of switching the enzyme between two forms. In this model, the metal ion need not change rate constants for the chemical transformations catalyzed by the enzyme; its role is simply to change the equilibrium constant for interconversion of the two forms. This more "structural" role is shown in the following reaction:

$$
\begin{array}{ccccc}
E(Ain) + M^+ & \rightleftharpoons & E(Aex_1) + M^+ & \rightleftharpoons & E(A\text{-}A) + M^+ \\
\updownarrow & & \updownarrow & & \updownarrow \\
E^*(Ain) + M^+ & \rightleftharpoons & E^*(Aex_1) + M^+ & \rightleftharpoons & E^*(A\text{-}A) + M^+ \\
\updownarrow & & \updownarrow & & \updownarrow \\
(M^+)E^*(Ain) & \rightleftharpoons & (M^+)E^*(Aex_1) & \rightleftharpoons & (M^+)E^*(A\text{-}A)
\end{array}
\tag{14}
$$

Both types of model have been tested by simulating the reaction time courses for the reaction of $\alpha_2\beta_2$ with L-Ser. Each model is able to reproduce both the effects on relaxation rates and the different amplitudes of transient E(Aex1) formation. In both models, the monovalent metal ion is an intricate part of catalysis that functions to maintain the enzyme in its active form. Since metal ion binding obviously also plays a crucial role in the allosteric cross-talk between subunits, a change in conformation,

either metal ion induced or metal ion driven through equilibrium shifts, must be an important part of the model. A three-dimensional structure of the tryptophan synthase bienzyme complex in the presence of monovalent metal ion is currently under investigation [143]. The successful completion of this work should give new insights into the specific role played by monovalent metal ions in tryptophan synthase catalysis.

5. Conclusions

The emerging X-ray structural information on MMA enzymes establishes that monovalent cations mediate catalytic activity via interactions at sites which are distinctly separate from the catalytic site and, hence, function as effectors of biological activity. The extensive literature on the structures and selectivity of small molecule complexes with the group I metal ions provides a rich body of information relevant to structure–function issues of importance to MMA enzymes. The crystallographic work on DGD [4,5,118] provides structural evidence showing that the switch between the inactive Na^+ complex and the active K^+ complex is a consequence of conformation change in the protein that is brought about by the change in ion size, and attendant change in coordination geometry at the metal site, which triggers a large change in protein conformation that alters the catalytic site. While the structural work is not quite as advanced for tryptophanase, TPL or tryptophan synthase, it seems likely that the effects of metal ions on these enzymes will have similar conformational origins. Solution studies of several MMA enzymes [22,28–31,50,51] indicate that the mechanisms of metal-ion-induced activation involve dynamic interactions between the metal ion and the protein that selectively alter the energies of both the ground state and the transition state of some steps in the catalytic cycle by selectively binding to the protein conformations that are complementary to these activated complexes. Accordingly, one role of monovalent metal ion activation is to drive protein conformational transitions necessary to achieve complementarity between the site and the activated complex.

Although considerable progress has been made toward a detailed understanding of the relationship between structure and function in MMA enzymes by the recently solved X-ray structures [4–10,34] and by detailed solution studies [22–31,50,51], there remain many unanswered questions about the mechanism. For example, in the MMA PLP enzyme systems, it is not yet clear how or whether monovalent metal ion activation is linked to conformational transitions which drive enzyme-bound intermediates to structures where the bond to be cleaved (or formed) is properly aligned with the PLP ring π system (Dunathan's hypothesis [109,110]). However, the remarkable dependence of quinonoid formation on the binding of an activating metal ion in the tryptophanase [19,22], TPL [27] and tryptophan synthase [30,31] systems strongly suggests that orbital alignment is linked to metal ion binding. In the tryptophan synthase system, metal ion binding is essential for establishing communication between the α and β sites [30,31]. However, the nature of the structural interactions and the raison d'être for involving the metal site in this allosteric

interaction is unknown. Because the concentrations of the free monovalent metal ion (Na^+ or K^+) usually are well above the dissociation constants for metal ion binding, we have assumed throughout this review that, under physiological conditions, MMA enzymes exist in their metal-bound activated forms. However, the switch in some systems between inactive and active forms [4,5,19,22,27,34,50,51,118] accompanying the exchange of Na^+ and K^+ may indicate an underlying regulatory significance in vivo. It is our hope that, by preparing a review on the subject of MMA enzymes at this juncture, research will be stimulated in this interesting area of coordination chemistry and bioinorganic mechanism.

Acknowledgments

References

[1] C.H. Suelter, Science, 168 (1970) 789.
[2] C.H. Suelter, in H. Sigel (ed.), Metal Ions in Biological Systems, Marcel Dekker, New York, 1974. p. 201.
[3] H.J. Evans and G.J. Sorger, Annu. Rev. Plant Physiol., 17 (1966) 47.
[4] M.D. Toney, E. Hohenester, S.W. Cowan and J.N. Jansonius, Science, 261 (1993) 756.
[5] M.D. Toney, E. Hohenester, J.W. Keller and J.N. Jansonius, J. Mol. Biol., 245 (1995) 151.
[6] A.A. Antson, G.G. Dodoson, K.S. Wilson, S.V. Pletnev, E.G. Harutyunyan and T.V. Demidkina, in G. Mariro, G. Sannia and F. Bossa (eds.), Biochemistry of Vitamin B_6 and PQQ, Birkhauser, Basel, 1994. in press.
[7] A.A. Antson, personal communication, 1994.
[8] A.A. Antson, T.V. Demidkia, P. Gollnick, Z. Dauter, R.L. Von Tersch, J. Long, S.N. Berezhnoy, R.S. Phillips, E.H. Harutyunyan and K.S. Wilson, Biochemistry, 32 (1993) 4195.
[9] M.N. Isupov, A.A. Antson, G.G. Dodson, I.S. Dementieva, L.N. Zakomirdina and E.H. Harutyunyan, in G. Mariro, G. Sannia and F. Bossa (eds.), Biochemistry of Vitamin B_6 and PQQ, Birkhauser, Basel, 1994. in press.
[10] M.N. Isupov, personal communication, 1994.

[11] H.G. Aaslestad and A.D. Larson, J. Bacteriol., 88 (1964) 1296.

[12] G.B. Bailey and W.B. Dempsey, Biochemistry, 6 (1967) 1526.

[13] G.B. Bailey, O. Chotamangsa and K. Vuttivej, Biochemistry, 9 (1970) 3243.

[14] G.B. Bailey, T. Kusamrarn and K. Vuttivej, Fed. Proc., Fed. Am. Soc. Exp. Biol., 29 (1970) 857.

[15] H.G. Aaslestad, P.J. Bouis, Jr., A.T. Philips and A.D. Larson, in E.E. Snell, A.E. Braunstein, E.S. Severin and Y.M. Torchinsky (eds.), Pyridoxal Catalysis: Enzymes and Model Systems, Wiley Interscience, New York, 1968, p. 479.

[16] C.A. Lamartiniere, H. Itoh and W.B. Dempsey, Biochemistry, 10 (1971) 4783.

[17] M. Honma, M. Ikeda and T. Shimomura, Agric. Biol. Chem., 36 (1972) 1661.

[18] J.W. Keller, K.B. Baurick, G.C. Rutt, M.V. O'Malley, N.L. Sonafrank, R.A. Reynolds, L.O.E. Ebbesson and F.F. Vajdos, J. Biol. Chem., 265 (1990) 5531.

[19] Y. Morino and E.E. Snell, J. Biol. Chem., 242 (1967) 2800.

[20] Y. Morino and E.E. Snell, J. Biol. Chem., 242 (1967) 5591.

[21] A. Hogberg-Raibaud, O. Raibaud and M.E. Goldberg, J. Biol. Chem., 250 (1975) 3352.

[22] C.H. Suelter and E.E. Snell, J. Biol. Chem., 252 (1977) 1852.

[23] D.S. June, B. Kennedy, T.H. Pierce, S.V. Elias, F. Halaka, I. Behbahani-Nejad, A.E. Bayoumi, C.H. Suelter and J.L. Dye, J. Am. Chem. Soc., 101 (1979) 2218.

[24] C.M. Metzler, R. Viswanath and D.E. Metzler, J. Mol. Biol., 266 (1991) 9374.

[25] W.A. Newton and E.E. Snell, Proc. Natl. Acad. Sci. USA, 52 (1964) 382.

[26] R.S. Phillips, Biochemistry, 30 (1991) 5927.

[27] H. Chen and R.S. Phillips, Biochemistry, 32 (1993) 11591.

[28] A. Peracchi, A. Mozzarelli and G.L. Rossi, in G. Mariro, G. Sannia and F. Bossa (eds.), Biochemistry of Vitamin B$_6$ and PQQ, Birkhauser, Basal, 1994, in press.

[29] A. Peracchi, A. Mozzarelli and G.L. Rossi, submitted.

[30] M.F. Dunn, P.S. Brzovic', C.A. Leja, P. Pan and E.U. Woehl, in G. Mariro, G. Sannia and F. Bossa (eds.), Biochemistry of Vitamin B$_6$ and PQQ, Birkhauser, Basel, 1994, in press.

[31] E.U. Woehl and M.F. Dunn, Biochemistry, 34 (1995), in press.

[32] O. Gursky, Y. Li, J. Badger and D.L.D. Caspar, Biophys. J., 61 (1992) 604.

[33] J. Badger, A. Kapulsky, O. Gursky, B. Bhyravbhatla and D.L.D. Caspar, Biophys. J., 66 (1994) 286.

[34] T.M. Larson, L.T. Laughlin, H.M. Holden, I. Royment and G.H. Reed, Biochemistry, 33 (1994) 630.

[35] P.J. Koostra, K.H. Kalk and W.G.J. Hol, Eur. J. Biochem., 177 (1988) 345.

[36] L.J. Lijk, C.A. Trofs, K.H. Kalk, M.C.H. De Maeyer and W.G.J. Hol, Eur. J. Biochem., 142 (1984) 399.

[37] M.W. Pantoliano, M. Whitlow, J.F. Wood, M.L. Rollence, B.C. Finzel, G.L. Gilliland, T.L. Poulos and P.N. Bryan, Biochemistry, 27 (1988) 8311.

[38] C. Walsh, Enzymatic Reaction Mechanisms, Freeman, San Francisco, CA, 1977, p. 777.

[39] M.F. Dunn, Struct. Bonding (Berlin), 23 (1975) 61.

[40] M.F. Dunn, in G. Berthon (ed.) Handbook on Metal–Ligand Interactions (1994) in press.

[41] I. Bertini, C. Luchinat, W. Maret and M. Zeppezauer, Progress in Inorganic Biochemistry and Biophysics, Vol. 1, Birkhauser, Basle, 1986, p. 1.

[42] M.F. Perutz, Q. Rev. Biophys., 22 (1989) 139.

[43] B.W. Matthews, P.M. Coleman, J.N. Jansonius, K. Titani, K.A. Walsh and H. Neurath, Nature, New Biol., 238 (1972) 41.

[44] B.W. Matthews and L.H. Weaver, Biochemistry, 13 (1974) 1719.

[45] G. Voordouw and R.S. Roche, Biochemistry, 14 (1975) 4667.

[46] M. Epstein, A. Leviztki and J. Ruben, Biochemistry, 13 (1974) 1777.

[47] D. Gabel and V. Kasche, Acta Chem. Scand., 27 (1973) 1971.

[48] B.W. Matthews, L.H. Weaver and W.R. Kester, J. Biol. Chem., 249 (1974) 8030.

[49] C. Ramashandran, J. Gory, E. Waelkens, W. Merlevedes and D.A. Walsh, J. Biol. Chem., 262 (1987) 3210.

[50] C.M. Wells and E. Di Cera, Biochemistry, 31 (1992) 11721.

[51] F.C. Wedler and B.W. Ley, Arch. Biochem. Biophys., 301 (1993) 416.

[52] C.H. Suelter, J. Wang and E.E. Snell, Anal. Biochem., 76 (1976) 221.

[53] O. Raibaud and M.E. Goldberg, Eur. J. Biochem., 73 (1977) 591.

[54] M.N. Kazarinoff and E.E. Snell, J. Biol. Chem., 256 (1980) 6228.
[55] M. Tokiushige, N. Tsujimoto, T. Oda, T. Honda, N. Yumoto, S. Ito, M. Yamamoto, E.H. Kim and Y. Hiragi, Biochimie, 71 (1989) 711.
[56] S. Kimura, S. Asari, S. Hayashi, Y. Yamaguchi, R. Fushimi, N. Amino and K. Miyai, Clin. Chem., 38 (1992) 44.
[57] A.R. Fersht, Enzyme Structure and Mechanism, Freeman, New York, 2nd edn., 1985, p. 1.
[58] M.L. Bender, F.J. Kezdy and C.R. Gunter, J. Am. Chem. Soc., 86 (1964) 3714.
[59] H.L. Oppenheimer, B. Labouesse and G.P. Hess, J. Biol. Chem., 241 (1966) 2720.
[60] L. Pauling, Chem. Eng. News, 24 (1946) 1375.
[61] L. Pauling, Am. Sci., 36 (1948) 51.
[62] C.-I. Branden, H. Jornvall, H. Eklund and B. Furugren, in P.D. Boyer (ed.), The Enzymes XI, Academic Press, New York, 1975, pp. 103–190.
[63] C.A. McPhalen, M.G. Vincent, D. Picot, J.N. Jansonius, A.M. Lesk and C. Chothia, J. Mol. Biol., 227 (1992) 197.
[64] G. Eichele, G.C. Ford, M. Glor, J.N. Jansonius, D. Mavrides and P. Christen, J. Mol. Biol., 133 (179) 161.
[65] A. Arnone, P.H. Rogers, C.C. Hyde, P.D. Briley, C.M. Metzler and D.E. Metzler, in P. Christen and D.E. Metzler (eds.) Transaminases, Wiley, New York, 1985, p. 138.
[66] P. Christen and D.E. Metzler (eds.), Transaminases, Wiley, New York, 1985.
[67] C.M. Anderson, F.H. Zucker and T.A. Steitz, Science, 204 (1979) 3750.
[68] D.L. Pompliano, P. Anusch and J.R. Knowles, Biochemistry, 29 (1990) 3186.
[69] E. Lolis and G. Petsko, Biochemistry, 29 (1990) 6619.
[70] M. Wilmanns, C.C. Hyde, D.R. Davies, K. Kirschner and J.N. Jansonius, Biochemistry, 30 (1991) 9161.
[71] M.F. Dunn, V. Aguilar, P.S. Brzovic, W.F. Drewe Jr., K.F. Houben, C.A. Leja and M. Roy, Biochemistry, 29 (1990) 8598.
[72] P.S. Brzovic, Y. Sawa, C.C. Hyde, E.W. Miles and M.F. Dunn, J. Biol. Chem., 267 (1992) 13028.
[73] P.S. Brzovic, K. Ngo and M.F. Dunn, Biochemistry, 31 (1992) 3831.
[74] P.S. Brzovic, C.C. Hyde, E.W. Miles and M.F. Dunn, Biochemistry, 32 (1993) 10404.
[75] W.F. Drewe, Jr., and M.F. Dunn, Biochemistry, 24 (1985) 3977.
[76] W.F. Drewe, Jr., and M.F. Dunn, Biochemistry, 25 (1986) 2494.
[77] F.A. Cotton and G. Wilkinson, Advanced Inorganic Chemistry, Wiley, New York, 5th edn., 1988.
[78] A.G. Sharpe, Inorganic Chemistry, Longman Scientific and Technical, Harlow, Essex, 3rd edn., 1992, p. 226.
[79] A.V. Bajaj and N.S. Poona, Coord. Chem. Rev., 87 (1988) 55.
[80] R.M. Izatt, J.S. Bradshaw, S.A. Nielsen, J.D. Lamb and J.J. Christensen, Chem. Rev., 85 (1985) 271.
[81] M. Dobler, Ionophores and Their Structures, Wiley, New York, 1981, pp. 5, 39.
[82] D.J. Cram, Angew. Chem., 25 (1986) 1039.
[83] M. Dobler, J.D. Dunitz and B.T. Kilbourn, Helv. Chim. Acta, 52 (1969) 2573.
[84] M. Dobler, Helv. Chim. Acta, 55 (1972) 136.
[85] K. Neupert-Laves and M. Dobler, Helv. Chim. Acta, 59 (1976) 614.
[86] M. Dobler and R.P. Phizackerley, Helv. Chim. Acta, 57 (1974) 664.
[87] T.J. Marrone and K.M. Merz, Jr., J. Am. Chem. Soc., 114 (1992) 754.
[88] Y. Barrans, M. Alleaume and L. David, Acta Crystallogr., Sect. B, 36 (1980) 936.
[89] J.-C. Beloeil, V. Biou, G. Dauphin, J. Garner, N. Morellet and F. Vaufrey, Magn. Reson. Chem., 32 (1994) 83.
[90] R.D. Shannon, Acta Crystallogr., Sect. A,32 (1976) 751.
[91] D.J. Cram, T. Kaneda, R.C. Helgeson, S.B. Brown, C.B. Knobler, E. Maverick and K.N. Trueblood, J. Am. Chem. Soc., 107 (1985) 3645.
[92] D.J. Cram and G.M. Lein, J. Am. Chem. Soc., 107 (1985) 3657.
[93] D.J. Cram, S.P. Ho, C.B. Knobler, E. Maverick and K.N. Trueblood, J. Am. Chem. Soc., 108 (1986) 2989.
[94] D.J. Cram and S.P. Ho, J. Am. Chem. Soc., 108 (1986) 2998.

[95] D.J. Cram, R.A. Carmack, M.P. deGrandpre, G.M. Lein, I. Goldberg, C.B. Knobler, E.F. Maverick and K.N. Trueblood, J. Am. Chem. Soc., 109 (1987) 7068.

[96] R.C. Helgeson, B.P. Czech, E. Chapoteau, C.R. Gebauer, A. Kumar and D.J. Cram, J. Am. Chem. Soc., 111 (1989) 6339.

[97] R.C. Helgeson, B.J. Selle, I. Goldberg, C.B. Knobler and D.J. Cram, J. Am. Chem. Soc., 115 (1993) 11 506.

[98] D.N. Reinhoudt and P.J. Dijkstra, Pure Appl. Chem., 60 (1988) 477.

[99] F.W. Alexander, E. Sandmeier, P.K. Mehta and P. Christen, Eur. J. Biochem. 219 (1994) 953.

[100] E.E. Snell and S.J. Dimari, in P.D. Boyer (ed.), The Enzymes II, Academic Press, New York, 1970, p. 335.

[101] C. Yanofsky and I.P. Crawford, in P.D. Boyer (ed.), The Enzymes VIII, Academic Press, New York, 34th edn., 1972, p. 1.

[102] E.W. Miles, Adv. Enzymol., 49 (1979) 127–186.

[103] D.E. Metzler, Adv. Enzymol., 50 (1979) 1–40.

[104] O. Hayaishi, Y. Ishimura and R. Kido (eds.), Biochemical and Medical Aspects of Tryptophan Metabolism, North-Holland, Amsterdam, 1980.

[105] J.F. Kirsch, G. Eichele, G.C. Ford, M.G. Vincent, J.N. Jansonius, H. Gehring and P. Christen, J. Mol. Biol., 174 (1984) 497.

[106] E.W. Miles, in D. Dolphin, R. Poulson and O. Avramovic (eds.), Pyridoxal Phosphate Enzymes Catalyzing β-Elimination and β-Replacement Reactions in Pyridoxal Phosphate and Derivatives, Coenzymes and Cofactors, Vol. I, Wiley, New York, 1986, p. 253.

[107] J.N. Jansonius and M.G. Vincent, in F.A. Jurnak and A. McPherson (eds.), Biological Macromolecules and Assemblies, Vol. 3, Wiley, New York, 1987, p. 187.

[108] E.E. Snell, Adv. Enzymol., 2 (1975) 287.

[109] H.C. Dunathan, Proc. Natl. Acad. Sci. USA, 55 (1966) 712.

[110] H.C. Dunathan, Adv. Enzymol., 35 (1971) 79–134.

[111] P.S. Brzovic' and M.F. Dunn, in H. Flores, J. Shannon and B. Singh (eds.), Biosynthesis and Molecular Regulation of Amino Acids in Plants, American Society of Plant Physiologists, Rockville, MD, USA, 1992, p. 37.

[112] D.M. Kiick and R.S. Phillips, Biochemistry, 27 (1988) 7339.

[113] D.S. June, C.H. Suelter and J.L. Dye, Biochemistry, 20 (1981) 2707.

[114] F.C. Happold and A. Struyvenberg, Biochem. J., 58 (1954) 379.

[115] W.A. Newton and E.E. Snell, Proc. Natl. Acad. Sci. USA, 51 (1964) 382.

[116] D.M. Kiick and R.S. Phillips, Biochemistry, 27 (1988) 7333.

[117] I.V. Myagkikh and T.V. Demidkina, Mol. Biol. (Kiev), 19 (1985) 671.

[118] E. Hohenester, J.W. Keller and J.N. Jansonius, Biochemistry, 33 (1994) 13561.

[119] J.P. Glusker, Adv. Protein Chem., 42 (1991) 1–76.

[120] C.C. Hyde, E.A. Padlan, S.A. Ahmed, E.W. Miles and D.R. Davies, J. Biol. Chem., 263 (1988) 17857.

[121] C.C. Hyde and E.W. Miles, Biotechnology, 8 (1990) 27.

[122] K.F. Houben and M.F. Dunn, Biochemistry, 29 (1990) 2421.

[123] A.N. Lane and K. Kirschner, Biochemistry, 30 (1991) 479.

[124] K. Kirschner, W. Weischet and R.L. Wiskocil, in H. Sund and G. Blaver (eds.), Protein–Ligand Interactions, Gruyter, Berlin, 1975, p. 27.

[125] A.N. Lane and K. Kirschner, Eur. J. Biochem., 120 (1981) 379.

[126] H. Kawasaki, R. Baurle, G. Zon, S.A. Ahmed and E.S. Miles, J. Biol. Chem., 262 (1987) 10678.

[127] K.S. Anderson, E.W. Miles and K.A. Johnson, J. Biol. Chem., 266 (1991) 8020.

[128] G. Strambini, P. Cioni, A. Peracchi and A. Mozzarelli, Biochemistry, 31 (1992) 7535.

[129] A. Mozzarelli, A. Peracchi, S. Bettati and G.L. Rossi, Proc. 8th Int. Congress on Vitamin B6 and Carbonyl Catalysis, Pergamon, Oxford, 1991, p. 273.

[130] M. Hatanaka, E.A. White, K. Horibata and I.P. Crawford, Arch. Biochem. Biophys., 97 (1962) 596.

[131] I.P. Crawford and J. Ito, Proc. Natl. Acad. Sci. USA, 51 (1964) 390.

[132] M.E. Goldberg, S.S. York and L. Stryer, Biochemistry, 7 (1968) 3662.

[133] S.S. York, Biochemistry, 11 (1972) 2733.

[134] E.W. Miles and H. Kumagai, J. Biol. Chem., 249 (1974) 2843.

[135] X.-J. Yang and E.W. Miles. J. Biol. Chem., 267 (1992) 7520.

[136] S.A. Ahmed, C.C. Hyde, G. Thomas and E.W. Miles, Biochemistry, 26 (1987) 5492.

[137] A. Mozzarelli, A. Peracchi, G.L. Rossi, S.A. Ahmed and E.W. Miles, J. Biol. Chem., 264 (1989) 15774.

[138] M. Roy, S. Kieblawi and M.F. Dunn, Biochemistry, 27 (1988) 6698.

[139] M. Roy, E.W. Miles, R.S. Phillips and M.F. Dunn, Biochemistry, 27 (1988) 8661.

[140] K.F. Houben, W. Kadima, M. Roy and M.F. Dunn, Biochemistry, 28 (1989) 4140.

[141] M.F. Dunn, M. Roy, B. Robustell and V. Aguilar, in T. Korpela and P. Christen (eds.), Proc. 1987 Int. Congr. on Chemical and Biological Aspects of Vitamaian B6 Catalysis, Birkhauser, Basel, 1987, p. 171.

[142] P. Pan and M.F. Dunn, unpublished results, 1995.

[143] E.W. Miles, personal communication, 1994.